Effective interaction for vanadium oxyhydrides $Sr_{n+1}V_nO_{2n+1}H_n$ ($n = 1$ and $n \to \infty$): A constrained-RPA study

Masayuki Ochi and Kazuhiko Kuroki
Department of Physics, Osaka University, Machikaneyama-cho, Toyonaka, Osaka 560-0043, Japan

(Received 22 February 2019; revised manuscript received 11 April 2019; published 23 April 2019)

Transition metal oxides have been one of the central objects in the studies of electron correlation effects because of their rich variety of physical properties mainly depending on the transition metal element. On the other hand, exploiting the anion degrees of freedom is less popular but can be another promising way to control properties of strongly correlated materials. In particular, oxyhydrides offer a unique playground of strongly correlated low-dimensional electronic structure, where the s orbitals of hydrogen breaks a chemical bond between the cation t_{2g} orbitals. In this study, we evaluate the effective interaction, i.e., the screened Coulomb interaction parameters in low-energy effective models, for vanadium oxyhydrides $Sr_{n+1}V_nO_{2n+1}H_n$ ($n = 1, \infty$) using the constrained-random-phase approximation (cRPA). We find that the effective interaction in the t_{2g} model, where only the t_{2g} orbitals are explicitly considered, is strongly screened by the e_g bands compared with that for oxides, because the e_g bands are very entangled with the t_{2g} bands in the oxyhydrides. On the other hand, the effective interaction is rather strong in the d model, where all the vanadium d orbitals are explicitly considered, owing to a large energy separation between the V-d bands and the anion bands (O-p and H-s), because the O-p states are stabilized by the existence of the hydrogen atoms. These findings suggest that nontrivial and unique correlation effects can take place in vanadium oxyhydrides.

DOI: 10.1103/PhysRevB.99.155143

I. INTRODUCTION

Transition metal oxides are one of the most popular playgrounds for strong correlation effects [1]. For example, transition metal oxides with the Ruddlesden-Popper (RP) phase, $A_{n+1}B_nO_{3n+1}$ ($n = 1, 2, \ldots, \infty$) with B being a transition metal element, have a very simple layered crystal structure but exhibit several intriguing properties such as unconventional superconductivity in cuprates [2]. Physical properties of transition metal oxides are dominated mainly by the transition metal element. In addition, changing the A site element often alters materials properties, e.g., by the chemical pressure effect through the difference of its atomic radius, which sometimes induces a structural transition, and by the carrier doping effect through the difference of the valence number among A site elements, such as Sr^{2+} and La^{3+}.

An anion is another degree of freedom to control materials properties in transition metal oxides. For example, some kinds of cuprate superconductors with multiple anions, such as $La_2CuO_4F_x$ [3], $Nd_2CuO_{4-x}F_y$ [4], $Sr_2CuO_2F_{2+\delta}$ [5], and $(Ca_{1-x}Na_x)_2CuO_2Cl_2$ [6], exhibit a superconducting transition at several tens of kelvin. In these materials, fluorine or chlorine doping changes not only the carrier concentration but also the local environment around copper, which yields a different crystal field from oxides. Intercalated anions, e.g., fluorine atoms in $Sr_3Ru_2O_7F_2$ [7], can reduce the three dimensionality in layered structures by separating the layers along the stacked direction. Such compounds with multiple anions, named mixed-anion compounds, have recently attracted much attention owing to their possibilities of realizing novel functionalities in a different way from oxides [8].

In particular, among mixed-anion compounds, oxyhydrides are materials with unique and remarkable aspects because of the distinctive nature of hydrogen. For example, heavy electron doping enabled by hydrogen revealed two-dome superconducting phases neighboring with two different types of antiferromagnetic phases in $LaFeAsO_{1-x}H_x$ [9,10]. It is remarkable that several transition metal oxyhydrides have been reported in very recent years [11–22]. In vanadium oxyhydrides $Sr_{n+1}V_nO_{2n+1}H_n$ ($n = 1, 2, \infty$) [23,24], it was pointed out that chemical bonds among the V-t_{2g} orbitals through the O-p orbitals are partially lost when oxygen is partially replaced with hydrogen, because the H-s orbital has a different parity from the V-t_{2g} orbitals. Because hydrogen atoms are aligned in vanadium oxyhydrides [23,24], this role called a π blocker [25] decreases the dimensionality of the electronic structure. These studies also pointed out that the symmetry of the crystal field around vanadium is lowered by hydrogen.

Because $Sr_{n+1}V_nO_{3n+1}$ ($n = 1, \infty$) [Fig. 1(a) for $n = \infty$ and 1(c) for $n = 1$] have been a textbook compound for theoretical investigation of the electron correlation effects (e.g., Ref. [26]), it is important to study the electronic structure of the corresponding oxyhydrides $Sr_{n+1}V_nO_{2n+1}H_n$ ($n = 1, \infty$) [Figs. 1(b) and 1(d)]. This importance is also supported from experimental studies revealing that $Sr_{n+1}V_nO_{2n+1}H_n$ are strongly correlated materials. For example, an antiferromagnetic order with an anomalously reduced magnetic moment was observed for $n = 1, 2, \infty$ [23]. While the insulating state is realized at ambient pressure for $n = \infty$ [27], a metal-insulator transition is induced by applying pressure [25]. Although some studies reported first-principles electronic structure of $Sr_{n+1}V_nO_{2n+1}H_n$ calculated using density functional theory (DFT) and discussed their magnetic properties [25,28,29], more elaborate theoretical treatment of correlation

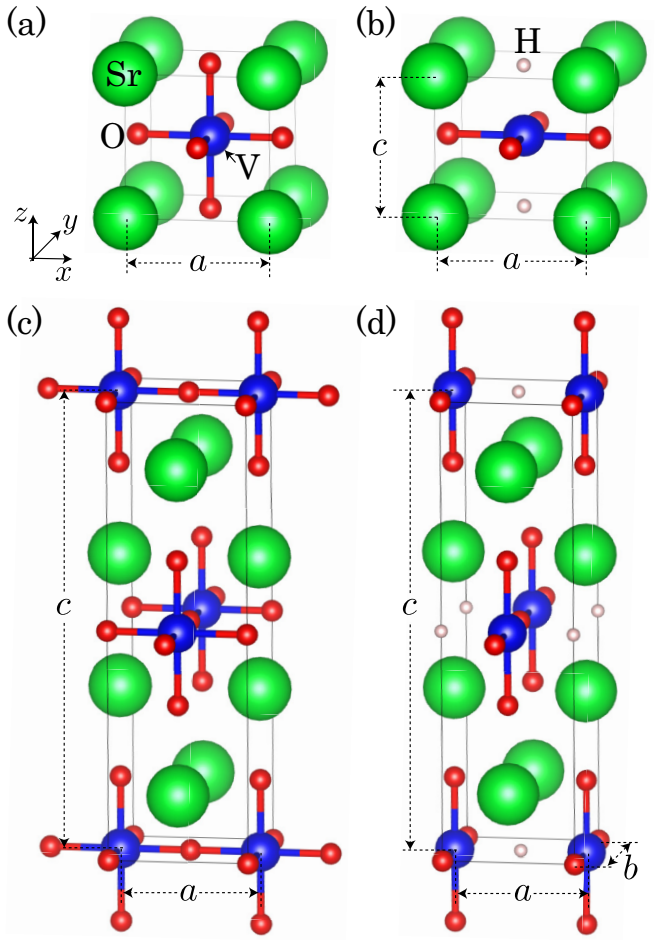

FIG. 1. Crystal structure of (a) $SrVO_3$, (b) $SrVO_2H$, (c) Sr_2VO_4, and (d) Sr_2VO_3H depicted using the VESTA software [32].

effects is often required for strongly correlated materials. For this purpose, it is essential to construct the model Hamiltonian representing the low-energy electronic structure, including the evaluation of the effective Coulomb interaction parameters, by first-principles calculation [30]. However, first-principles evaluation of such parameters for oxyhydrides has still been missing. We note that, although the magnetic interaction parameters calculated by the DFT + U method as presented in Refs. [28] and [29] are helpful for understanding the anisotropy of the magnetic interaction (i.e., when discussing their relative strength) in oxyhydrides, it is problematic that these parameters can vary by changing the U parameter assumed in the DFT+U calculations, in addition to the fact that the magnetic interaction is evaluated at the DFT level there.

In this study, we evaluate the screened Coulomb interaction parameters in low-energy effective models for $Sr_{n+1}V_nO_{2n+1}H_n$ ($n = 1, \infty$) using the constrained-random-phase approximation (cRPA) [31]. For this purpose, we start from the DFT band structure and verify the low-dimensional electronic structure in these materials as previous studies pointed out. As for the interaction parameters evaluated by cRPA, we find that the effective interaction in the V-t_{2g} model, where only the t_{2g} orbitals are explicitly considered, is sizably screened by the V-e_g bands because of strong entanglement between the t_{2g} and e_g bands. On the other hand, for the V-d model, where all the V-d orbitals are explicitly considered, the effective interaction is stronger than that for the oxides because of a large energy separation between the V-d bands and the anion bands (O-p and H-s). These findings suggest that possibly nontrivial and unique correlation effects can be realized in vanadium oxyhydrides, and also that special care must be taken in choosing which model to adopt in order to analyze the low-energy properties.

This paper is organized as follows: Section II presents a brief overview of the cRPA formulation, and some computational conditions are shown in Sec. III. Sections IV A and IV B present our calculation results for $n = \infty$ and $n = 1$ compounds, respectively. Our findings are summarized in Sec. V.

II. METHOD

We briefly review the formulation of cRPA, which was used to evaluate the interaction parameters of the low-energy effective models in our study. Because we concentrate on the static interaction, we show the cRPA formulation only for the static variables.

One begins with the Kohn-Sham orbitals ϕ_{kn} and their eigenvalues ϵ_{kn}, where $k = (\mathbf{k}, \sigma)$ is a combined index for the k vector and the spin σ and n is the band index. Then, the static independent-particle polarization function reads

$$\chi_0(\mathbf{r}, \mathbf{r}') = \sum_{kn}^{\text{occ.}} \sum_{k'n'}^{\text{unocc.}} \frac{1}{\epsilon_{kn} - \epsilon_{k'n'}} \times [\phi^*_{kn}(r)\phi_{k'n'}(r)\phi^*_{k'n'}(r')\phi_{kn}(r') + \phi^*_{kn}(r')\phi_{k'n'}(r')\phi^*_{k'n'}(r)\phi_{kn}(r)], \quad (1)$$

where kn and $k'n'$ are the indices of the occupied and unoccupied Kohn-Sham orbitals, respectively. In cRPA, one should exclude the electron excitations within the correlated subspace spanned by the Wannier orbitals (see Ref. [33] for more details about the treatment of the band entanglement). By denoting the rest of the polarization function as $\chi^r_0(\mathbf{r}, \mathbf{r}')$, the dielectric function ϵ in cRPA reads

$$\epsilon = 1 - v\chi^r_0, \quad (2)$$

where v is the bare Coulomb interaction. Finally, we obtain the screened Coulomb interaction,

$$W = \epsilon^{-1}v. \quad (3)$$

By using W, the effective interaction parameters between the Wannier functions $\psi_n(\mathbf{r})$ and $\psi_m(\mathbf{r})$ are evaluated as follows:

$$U^{\text{scr}}_{nm} = \int d\mathbf{r}d\mathbf{r}'|\psi_n(\mathbf{r})|^2 W(\mathbf{r}, \mathbf{r}')|\psi_m(\mathbf{r}')|^2, \quad (4)$$

$$J^{\text{scr}}_{nm} = \int d\mathbf{r}d\mathbf{r}'\psi^*_n(\mathbf{r})^2\psi_m(\mathbf{r})W(\mathbf{r}, \mathbf{r}')\psi_n(\mathbf{r}')\psi^*_m(\mathbf{r}'), \quad (5)$$

for the direct Coulomb and exchange interactions, respectively. When the screened interaction W^r in the above integrals is replaced with the bare interaction v, we shall denote these variables as U^{bare}_{nm} and J^{bare}_{nm}, respectively.

III. COMPUTATIONAL DETAILS

First, we calculated the first-principles band structure using the QUANTUM ESPRESSO code [34,35]. Perdew-Burke-Ernzerhof parametrization of the generalized gradient approximation (PBE-GGA) [36] and the scalar-relativistic version of the optimized norm-conserving Vanderbilt pseudopotentials [37] taken from PseudoDojo [38] were used. For the pseudopotentials, core electrons of each element are as follows: [He] for O, [Ne] for V and Cr, and [Ar]$3d^{10}$ for Sr (i.e., V-$3s^2 3p^6$ and Sr-$4s^2 4p^6$ semicore states are treated as valence). Experimental crystal structures were taken from Ref. [39] for $SrVO_3$, Ref. [23] (data taken at 5 K) for $SrVO_2H$, Ref. [24] for Sr_2VO_4 and Sr_2VO_3H, and Ref. [40] for $SrCrO_3$. The plane-wave cutoff energy of 150 Ry, a $12 \times 12 \times 12$ k mesh for $SrVO_3$, $SrVO_2H$, and $SrCrO_3$, and a $10 \times 10 \times 10$ k mesh for Sr_2VO_4 and Sr_2VO_3H were used with the Gaussian smearing width of 0.02 Ry.

Next, we extracted (maximally localized) Wannier functions [41,42] using the RESPACK code [43–47], by which we also obtained the hopping parameters among the Wannier functions. Finally, we evaluated the interaction parameters among the Wannier functions using cRPA [31] as implemented in the RESPACK code. For this purpose, the cutoff energy of the dielectric function was set to 40 Ry for all the compounds. The total number of bands (i.e., the sum of the numbers of the valence and conduction bands) considered in our cRPA calculation was 200 for $SrVO_3$, $SrVO_2H$, and $SrCrO_3$, and 400 for Sr_2VO_4 and Sr_2VO_3H, unless noted.

In this paper, the t_{2g}, d, dp, and dps models denote the low-energy effective models consisting of the V(Cr)-$d_{xy,yz,xz}$, V(Cr)-d, V-d + O-p, V-d + O-p + H-s orbitals, respectively. Although t_{2g} is an inappropriate name for oxyhydrides with a lowered crystal-field symmetry in the strict sense of the term, we call the $d_{xy,yz,xz}$ orbitals the "t_{2g} orbitals" for simplicity. We also call the remaining d orbitals the "e_g orbitals."

IV. RESULTS AND DISCUSSIONS

For all the compounds investigated in this study, we shall show their hopping and interaction parameters only partially in the main text. A more extensive list of these parameters is shown in Appendixes A and B.

A. $SrVO_3$ and $SrVO_2H$ ($n = \infty$)

1. Band structure and Wannier functions

Figure 2 presents the calculated electronic band structure of $SrVO_3$, $SrVO_2H$, and $SrCrO_3$. Here, we calculated the electronic structure of $SrVO_3$ to compare it with that for $SrVO_2H$. Because $SrVO_3$ and $SrVO_2H$ have different d-electron occupation numbers, d^1 for the former and d^2 for the latter, we also show some results for $SrCrO_3$ with d^2 configuration to enable more detailed comparison among them. In Fig. 2, the band structure calculated with the tight-binding model consisting of the Wannier functions are shown with red solid lines along with the first-principles one with black broken lines. The corresponding tight-binding models are the t_{2g} model in Figs. 2(a), 2(d) and 2(g), the d model in Figs. 2(b), 2(e) and 2(h), the dp model in Fig. 2(c), and the dps model in Fig. 2(f).

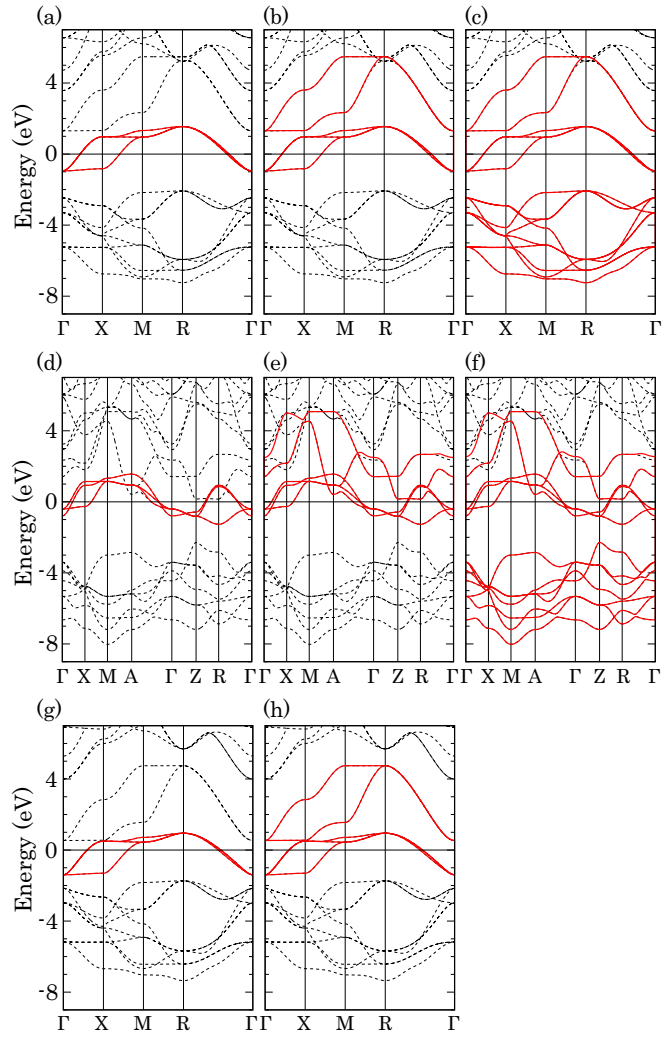

FIG. 2. Calculated electronic band structure of (a)–(c) $SrVO_3$, (d)–(f) $SrVO_2H$, and (g)–(h) $SrCrO_3$. First-principles band structure is shown with black broken lines and the band dispersion calculated with the tight-binding model consisting of the Wannier functions is shown with red solid lines. Corresponding effective models are t_{2g} for panels (a), (d), and (g), d for panels (b), (e), and (h), dp for panel (c), and dps for panel (f).

The band structure of $SrVO_2H$ is similar to but in part different from those for $SrVO_3$ and $SrCrO_3$. For example, the t_{2g} band dispersion along the Γ-X-M-A-Γ line in $SrVO_2H$, shown with red solid lines in Fig. 2(b), is very similar to that along the Γ-X-M-R-Γ line in the oxides, shown with red solid lines in Figs. 2(a) and 2(g). We note that both these two k paths represent $(0, 0, 0)$-$(\pi/a, 0, 0)$-$(\pi/a, \pi/a, 0)$-$(\pi/a, \pi/a, \pi/c)$-$(0, 0, 0)$ in the Cartesian coordinate, where a and c ($= a$ for the oxides) are the lattice constants shown in Figs. 1(a) and 1(b). On the other hand, the t_{2g} bands show a small dispersion along the k_z direction, such as along the Γ-Z line, for $SrVO_2H$, unlike the corresponding band dispersion in the oxides, i.e., those along the Γ-X line. Such a small band dispersion along the k_z direction is induced by the hydrogen atom placing along the z direction as shown in Fig. 1(b). In other words, the H-s orbital cannot form a chemical bond with the V-t_{2g} orbitals because of

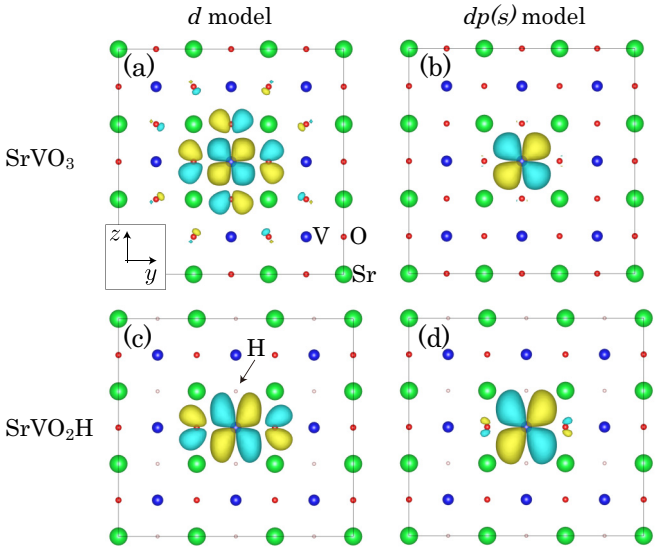

FIG. 3. Wannier orbitals of V-d_{yz} for (a),(b) $SrVO_3$ and (c),(d) $SrVO_2H$. Corresponding effective models are d for panels (a),(c), dp for panel (b), and dps for panel (d).

their different parities [23,24]. Such a low dimensionality is characteristic of oxyhydrides.

To see the low dimensionality of the t_{2g} states in more detail, we depicted the d_{yz} Wannier orbitals in Fig. 3. As is consistent with the previous theoretical study [29], the t_{2g} Wannier orbital in the t_{2g} or d models (the former not shown here), which can be usually regarded as an antibonding pair of the atomic orbitals of the cation and the surrounding anions, has no weight on hydrogen sites. It is also noteworthy that the t_{2g} orbital tends to extend in $SrVO_2H$ [29]. This feature is maintained also in the $dp(s)$ model as shown in Figs. 3(b) and 3(d), suggesting that this delocalization is partially brought by

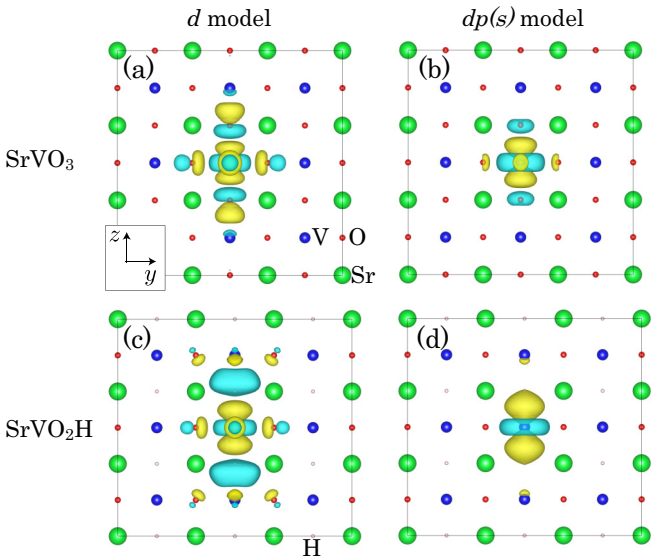

FIG. 4. Wannier orbitals of V-$d_{3z^2-r^2}$ for (a),(b) $SrVO_3$ and (c),(d) $SrVO_2H$. Corresponding effective models are d for panels (a),(c), dp for panel (b), and dps for panel (d).

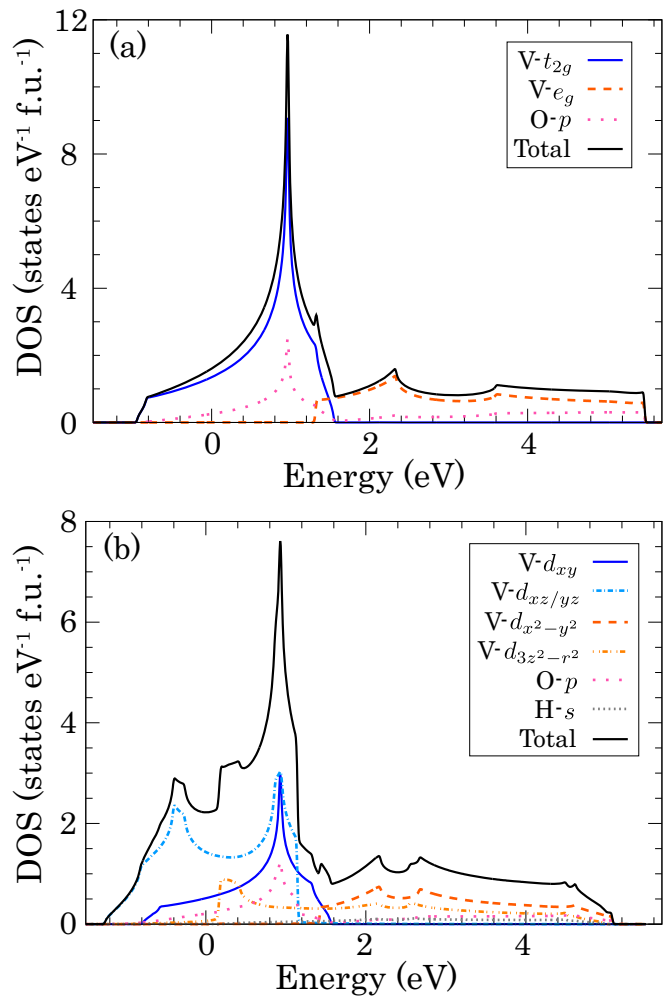

FIG. 5. (Partial) DOS for (a) $SrVO_3$ and (b) $SrVO_2H$ calculated with our $dp(s)$ tight-binding model.

a lower-energy crystal field in $SrVO_2H$, where O^{2-} is partially replaced with H^-.

Such a low dimensionality can also be seen in Fig. 5. While a shape of the density of states (DOS) characteristic of two-dimensional electronic structure on the square lattice can be seen for the t_{2g} orbitals in $SrVO_3$ and the d_{xy} orbital in $SrVO_2H$, a strong DOS enhancement near the band edge, which is characteristic of (quasi-)one-dimensional electronic structure, is realized for the $d_{xz/yz}$ orbitals in $SrVO_2H$.

While we mainly focused on the t_{2g} orbitals so far, the e_g orbitals in $SrVO_2H$, which can form a chemical bond with the H-s orbital as shown in Fig. 4(c), are also quite different from those in $SrVO_3$. For example, as shown in Fig. 2(e), the energy levels of the e_g bands in $SrVO_2H$ are much lowered by hydrogen compared with $SrVO_3$. As a result, the bottom of the e_g bands is very close to the Fermi energy in $SrVO_2H$, which can also be seen in Fig. 5(b). We shall come back to this point later in this paper.

2. Hopping parameters

A portion of the hopping parameters is shown in Tables I and II, where t_i $(i = x, y, z)$ denotes the nearest-neighbor

TABLE I. Hopping and interaction parameters (in eV) for the t_{2g} model. Equivalent orbitals to the listed ones, e.g., d_{xz} in $SrVO_2H$, are omitted in this table.

		t_x	t_y	t_z	Δ	$U^{\rm scr}_{t_{2g}}$	$U^{\rm bare}_{t_{2g}}$
$SrVO_3$	d_{xy}	−0.26	−0.26	−0.03		3.42	15.78
						3.48 [43]	
						3.2 [48]	16.1 [48]
						3.39 [49]	15.0 [49]
						3.36 [49]	16.0 [49]
						3.4 [50]	
						3.3 [51]	
$SrVO_2H$	d_{xy}	−0.25	−0.25	−0.04		3.00	16.04
	d_{yz}	0.01	−0.42	0.10	−0.45	2.60	15.18
$SrCrO_3$	d_{xy}	−0.24	−0.24	−0.02		2.97	16.18
						2.7 [48]	16.4 [48]

hopping parameter along the i direction between the same type of the orbital (e.g., d_{yz}-d_{yz}), and Δ is the on-site energy relative to the d_{xy} orbital. We note that these parameters are not sufficient to reproduce the first-principles band structure. We just show them to discuss the dimensionality of the electronic structure. A set of the hopping parameters for the t_{2g} and d models that can well reproduce the band dispersion are provided in Appendix A.

In Table I, we can see that the hopping parameters for the d_{xy} orbital are almost the same among $SrVO_3$, $SrVO_2H$, and $SrCrO_3$. On the other hand, hydrogen atoms yield a drastically suppressed value of t_z, −0.04 eV, for the $d_{xz/yz}$ orbitals in $SrVO_2H$. As a result, the quasi-one-dimensional electronic structure is realized for the $d_{xz/yz}$ orbitals in $SrVO_2H$ as we have seen in the previous section. In the previous section, we have also mentioned that a sizably increased value of t_y for the d_{yz} orbital (t_x for the d_{xz} orbital) in $SrVO_2H$ (−0.42 eV) from that in $SrVO_3$ (−0.26 eV) is another characteristic feature of oxyhydrides, which was pointed out in the previous theoretical study on $SrCrO_2H$ with a hypothetically hydrogen-ordered structure [29]. This feature also enhances the low dimensionality of the $d_{xz/yz}$ states in $SrVO_2H$. The crystal-field splitting induced by hydrogen can be seen in Table I: the on-site energy of the $d_{xz/yz}$ orbitals relative to the d_{xy} orbital becomes a sizable negative value (−0.45 eV) in $SrVO_2H$. All the features of the hopping parameters for the t_{2g} orbitals mentioned above are maintained also in the d model, as shown in Table II.

TABLE II. Hopping and interaction parameters (in eV) for the d model. Equivalent orbitals to the listed ones are omitted in this table.

		t_x	t_y	t_z	Δ	$U^{\rm scr}_{d}$	$U^{\rm bare}_{d}$
$SrVO_3$	d_{xy}	−0.26	−0.26	−0.02		3.43	15.85
						3.5 [52]	
	$d_{x^2-y^2}$	−0.51	−0.51	0.00	2.76	3.57	16.36
	$d_{3z^2-r^2}$	−0.17	−0.17	−0.67	2.76	3.57	16.36
$SrVO_2H$	d_{xy}	−0.25	−0.25	−0.04		3.97	16.06
	d_{yz}	0.01	−0.42	0.10	−0.44	3.75	15.28
	$d_{x^2-y^2}$	−0.44	−0.44	0.01	2.49	4.04	16.37
	$d_{3z^2-r^2}$	−0.09	−0.09	0.88	1.52	3.26	13.58
$SrCrO_3$	d_{xy}	−0.24	−0.24	−0.02		3.04	16.20
	$d_{x^2-y^2}$	−0.51	−0.51	0.00	2.52	3.18	16.82
	$d_{3z^2-r^2}$	−0.17	−0.17	−0.68	2.52	3.18	16.82

In Table II, we can see that the $d_{3z^2-r^2}$ orbital in $SrVO_2H$, which has a strong chemical bond with the H-s orbital as shown in Fig. 4(c), exhibits an enhanced value of t_z (0.88 eV) together with a lowered on-site energy (∼1 eV lower than that for the $d_{x^2-y^2}$ orbital). The sign of t_z for the $d_{3z^2-r^2}$ orbital is changed from the oxides to oxyhydride, which originates from the different parity of the O-p_z orbital in oxides and the H-s orbital in oxyhydride.

3. On-site direct Coulomb interaction

We next move on to the effective Coulomb interaction parameters obtained by our cRPA calculation. We start from the $dp(s)$ model because the screening processes taken into account are most limited there. The screened interaction for the on-site direct Coulomb terms among the V-d orbitals in $SrVO_3$ is

$$U^{\rm scr}_{dp} = \begin{pmatrix} 11.41 & 10.01 & 10.01 & 11.02 & 10.31 \\ 10.01 & 11.41 & 10.01 & 10.49 & 10.84 \\ 10.01 & 10.01 & 11.41 & 10.49 & 10.84 \\ 11.02 & 10.49 & 10.49 & 12.64 & 10.83 \\ 10.31 & 10.84 & 10.84 & 10.83 & 12.64 \end{pmatrix}, \tag{6}$$

while the bare interaction is

$$U^{\rm bare}_{dp} = \begin{pmatrix} 19.36 & 17.72 & 17.72 & 19.28 & 18.28 \\ 17.72 & 19.36 & 17.72 & 18.53 & 19.03 \\ 17.72 & 17.72 & 19.36 & 18.53 & 19.03 \\ 19.28 & 18.53 & 18.53 & 21.31 & 19.16 \\ 18.28 & 19.03 & 19.03 & 19.16 & 21.31 \end{pmatrix}, \tag{7}$$

where the orbital index runs as d_{xy}, d_{yz}, d_{xz}, $d_{x^2-y^2}$, and $d_{3z^2-r^2}$. For $SrVO_2H$, we obtained

$$U^{\rm scr}_{dps} = \begin{pmatrix} 8.16 & 6.48 & 6.48 & 7.61 & 6.53 \\ 6.48 & 7.28 & 6.17 & 6.72 & 6.65 \\ 6.48 & 6.17 & 7.28 & 6.72 & 6.65 \\ 7.61 & 6.72 & 6.72 & 8.95 & 6.79 \\ 6.53 & 6.65 & 6.65 & 6.79 & 7.90 \end{pmatrix}, \tag{8}$$

and

$$U^{\rm bare}_{dps} = \begin{pmatrix} 18.59 & 16.32 & 16.32 & 18.57 & 16.59 \\ 16.32 & 17.02 & 15.67 & 17.06 & 16.58 \\ 16.32 & 15.67 & 17.02 & 17.06 & 16.58 \\ 18.57 & 17.06 & 17.06 & 20.55 & 17.39 \\ 16.59 & 16.58 & 16.58 & 17.39 & 18.26 \end{pmatrix}. \tag{9}$$

Here, we omit other matrix elements such as d-p interaction, which are shown in Appendixes B 1 and B 2.

From these results, we found that the screened interaction in the $dp(s)$ model is much smaller for $SrVO_2H$ than that for $SrVO_3$. One of the reasons is the extended character of the Wannier functions in $SrVO_2H$ as we have seen, which can be inferred from the smaller bare interaction $U^{\rm bare}_{dps}$ in $SrVO_2H$ than $U^{\rm bare}_{dp}$ in $SrVO_3$. Another reason is the fact that there are many high-energy bands close to the V-d bands in $SrVO_2H$ as shown in Fig. 6(b), compared with $SrVO_3$ as shown in

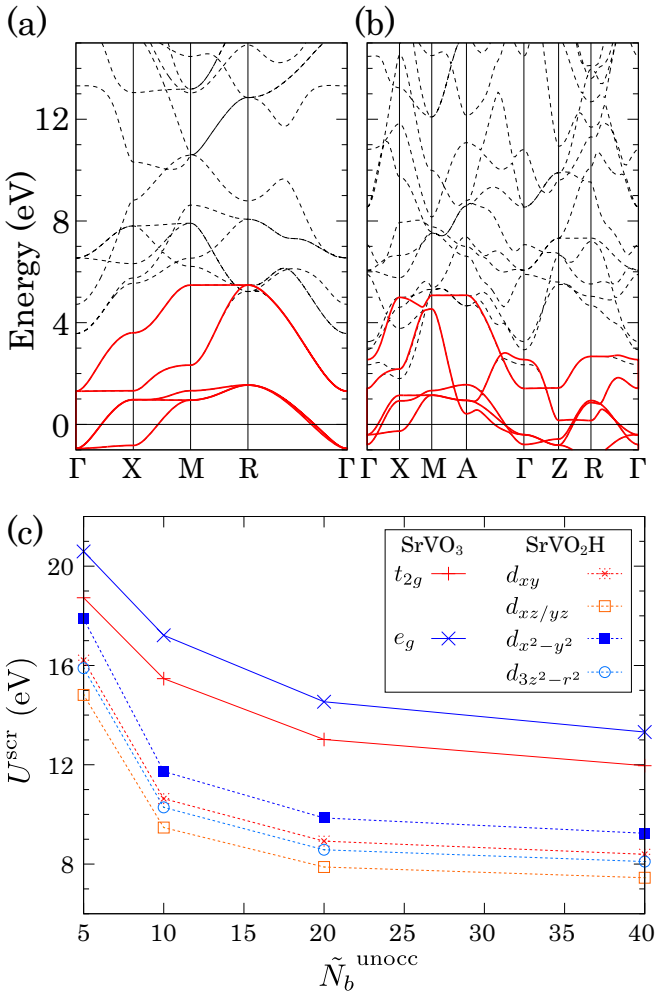

FIG. 6. (a) High-energy region of the electronic band structure for $SrVO_3$ shown in Fig. 2(c). (b) The same plot for $SrVO_2H$, i.e., Fig. 2(f). (c) $\tilde{N}_b^{\rm unocc}$ dependence of the screened interaction parameter $U^{\rm scr}$ in the $dp(s)$ model. The definition of $\tilde{N}_b^{\rm unocc}$ is given in the main text.

Fig. 6(a). Such high-energy bands close to the V-d bands can have a large contribution to the screening process.

To verify this issue, we calculated the screened interaction $U^{\rm scr}_{dp(s)}$ with changing the number of bands taken into account in cRPA calculations as shown in Fig. 6(c). Here, $\tilde{N}_b^{\rm unocc}$ roughly corresponds to the number of (partially) unoccupied bands including the V-3d bands. To be more precise, when one considers the screening processes within the lowest N_b bands, $\tilde{N}_b^{\rm unocc}$ is defined as N_b subtracted with 20 (i.e., a half of the number of electrons for Sr-4s4p, V-3s3p, and O-2s2p) in $SrVO_3$ and 17 (i.e., a half of the number of electrons for Sr-4s4p, V-3s3p, O-2s2p, and H-1s) in $SrVO_2H$. A sharp drop of $U^{\rm scr}$ at small $\tilde{N}_b^{\rm unocc}$ for $SrVO_2H$, as shown in Fig. 6(c), suggests that the strong entanglement of the V-d bands and higher-energy bands in $SrVO_2H$ is important for the strong screening effects.

For the d model, the screened Coulomb interaction among t_{2g} orbitals in $SrVO_2H$ now becomes stronger than $SrVO_3$, as shown in Table II. The difference between the d and $dp(s)$ models should come from the screening effects by the O-p and H-s orbitals: i.e., these anion orbitals weakly screen the Coulomb interaction among the V-d orbitals in $SrVO_2H$ compared with $SrVO_3$. This is naturally expected by the band dispersion shown in Figs. 2(b) and 2(e), where the anion bands are more separated from the V-d bands in $SrVO_2H$ than $SrVO_3$. In fact, the stronger screening effect in $SrCrO_3$ than $SrVO_3$ shown in Tables I and II originates from a smaller energy difference between the O-p and V(Cr)-d bands, as pointed out in Ref. [48]. Here, the lower on-site energy of Cr-d than that for V-d owing to the increased nuclear charge for Cr is the origin of such a small energy difference in $SrCrO_3$. It was theoretically pointed out that a similar situation was realized also in cuprates, where the longer the bond distance between apical oxygen and copper is, the stronger the screening effect becomes owing to a smaller d-p energy-level deference by stabilization of the copper d orbitals [53]. As for $SrVO_2H$, the large energy separation between the anion bands and the V-d bands is likely to come from the fact that the O-p orbitals are more stabilized by the existence of hydrogen atoms compared with the V-d orbitals. As a matter of fact, the on-site energy difference between the V-d_{yz} and O-p_z orbitals in the $dp(s)$ model for $SrVO_3$ and $SrVO_2H$ is 3.31 and 3.97 eV, respectively. It is also important that the number of the O-p bands is reduced in $SrVO_2H$ from $SrVO_3$. As for the e_g orbitals, it is noteworthy that both the bare and screened Coulomb interaction parameters are weak for the $d_{3z^2-r^2}$ orbitals in $SrVO_2H$ as shown in Table II, because of its extended nature that we have seen in previous sections.

Finally, we come to the t_{2g} model. The effective interaction in $SrVO_2H$ is again, as in the $dp(s)$ model, smaller than that in $SrVO_3$, likely because of the strong entanglement among the t_{2g} and e_g bands. In other words, the e_g orbitals strongly screen the effective interaction among the t_{2g} orbitals in $SrVO_2H$. In fact, the difference between $U^{\rm scr}_{t_{2g}}$ and $U^{\rm scr}_{d}$ is negligible in $SrVO_3$ (3.42 and 3.43 eV), very small in $SrCrO_3$ (2.97 and 3.04 eV) where the t_{2g} and e_g bands are slightly entangled, and quite large in $SrVO_2H$ (3.00 and 3.97 eV for d_{xy}, 2.60 and 3.75 eV for $d_{xz/yz}$) where the t_{2g} and e_g bands are strongly entangled. We note that the bare Coulomb interaction $U^{\rm bare}_{t_{2g}}$ and $U^{\rm bare}_{d}$ are rather close in $SrVO_2H$: 16.04 and 16.06 eV for d_{xy}, 15.18 and 15.28 eV for $d_{xz/yz}$, which rules out the possibility that the difference between $U^{\rm scr}_{t_{2g}}$ and $U^{\rm scr}_{d}$ comes from the variation of the Wannier orbitals (e.g., the size of the spread).

We summarize the complicated screening effects in $SrVO_2H$. The e_g bands strongly entangled with the t_{2g} bands sizably screen the effective interaction in the t_{2g} model. The large energy separation between the anion bands and the V-d bands weakens the screening effect by the anion orbitals in the d model (and the t_{2g} model). The strong entanglement of the V-d bands and higher-energy bands yields the strong screening effect in the dps model (and other two effective models). It is noteworthy that the different d-electron numbers between $SrVO_2H$ and $SrVO_3$ should play some role for making interaction parameters of these two systems different. As a matter of fact, in Ref. [49], the screened interaction (U, U', J) for the t_{2g} model in $SrVO_3$ evaluated using cRPA was reported to be (3.39, 2.34, 0.47) for the d^1 filling and (3.65, 2.59, 0.46) for the d^2 filling. Because the change in U and

U' is roughly 0.25 eV here, we can expect that the change in the band structure we have discussed above is still crucial for understanding the peculiar effective interaction in $SrVO_2H$ compared with $SrVO_3$.

Because of the sizable difference in effective interaction parameters among the t_{2g} and d models, it is a nontrivial issue which effective model one should adopt for analyzing the electronic structure of $SrVO_2H$. The lowered energy of the $d_{3z^2-r^2}$ bands, which comes close to the Fermi energy as shown in Fig. 2(e), might have some relevance to this issue. We also note that one possible origin of the large difference in the interaction parameters is the difficulty in evaluating χ_0^r when the band entanglement takes place. For treating the band entanglement, while we used the method shown in Ref. [33] as implemented in the RESPACK code, there is another choice such as the one shown in Ref. [54]. When the metallic screening is not fully removed by using the former method, the interaction parameters will become small (i.e., overscreened), which can be related to the case of the t_{2g} model in $SrVO_2H$. These are important future problems.

4. Off-site direct Coulomb interaction

We found that the off-site direct Coulomb interaction parameters exhibit a similar tendency to the on-site parameters for each model. For example, the screened interaction parameters of the nearest-neighbor off-site direct Coulomb interaction along the z direction for the d model are (0.58, 0.74) eV in $SrVO_3$ and (0.72, 0.83) eV in $SrVO_2H$, where the orbital-diagonal components of the interaction parameters for the d_{xy} and $d_{xz/yz}$ orbitals are shown. Similarly to the on-site terms, the effective off-site interaction in $SrVO_2H$ is stronger than that in $SrVO_3$ for the d model. On the other hand, the corresponding off-site interaction parameters become (0.58, 0.74) eV in $SrVO_3$ and (0.27, 0.33) eV in $SrVO_2H$, for the t_{2g} model, where the on-site screened interaction in $SrVO_2H$ is also weaker than that in $SrVO_3$. The above results might come from the fact that it is unchanged which electron excitations tend to play a major role in the screening process, irrespective of whether they are on-site or off-site interactions.

5. Exchange interaction

Unlike other parameters, the exchange interaction J is less sensitive to the existence of hydrogen atoms. For example, $J_{t_{2g}}^{\rm scr}$ is 0.48 eV for $SrVO_3$, while it is 0.46 between the d_{xy} and $d_{xz/yz}$ orbitals, and 0.42 between the d_{xz} and d_{yz} orbitals, for $SrVO_2H$. An unusual aspect of $SrVO_2H$ is a relatively large off-site screened exchange interaction between $d_{3z^2-r^2}$ and H-s in the dps model, 0.16 eV, while all the other off-site screened exchange interaction is less than 0.1 eV in $SrVO_3$ and $SrVO_2H$. This might be due to the large overlap of these two orbitals and the shortened lattice constant along the z direction.

B. Sr_2VO_4 and Sr_2VO_3H ($n = 1$)

For Sr_2VO_4 and Sr_2VO_3H ($n = 1$), we considered the $d_{y^2-z^2}$ and $d_{3x^2-r^2}$ orbitals as the e_g orbitals, instead of the $d_{x^2-y^2}$ and $d_{3z^2-r^2}$ orbitals. This is because hydrogen atoms make the x axis quite inequivalent from other axes in Sr_2VO_3H, as shown in Fig. 1(d).

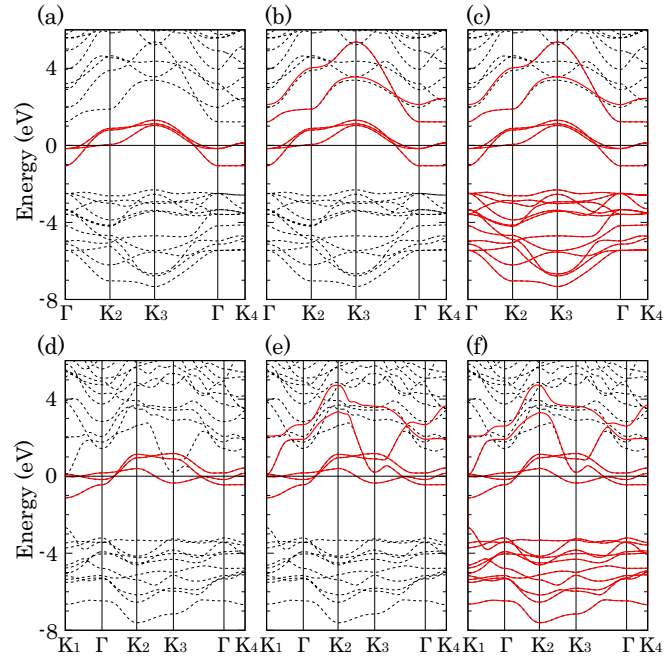

FIG. 7. Calculated electronic band structure of (a)–(c) Sr_2VO_4 and (d)–(f) Sr_2VO_3H. First-principles band structure is shown with black broken lines and the band dispersion calculated with the tight-binding model consisting of the Wannier functions is shown with red solid lines. Corresponding effective models are t_{2g} for panels (a) and (d), d for panels (b) and (e), dp for panel (c), and dps for panel (f). To compare the band structures of Sr_2VO_4 and Sr_2VO_3H, common special k points were taken as follows: $K_1 = (\pi/a, 0, 0)$, $K_2 = (0, \pi/b, 0)$, $K_3 = (\pi/a, \pi/b, 0)$, and $K_4 = (0, 0, 2\pi/c)$ in the Cartesian coordinate, where a, b ($= a$ for Sr_2VO_4), and c are the lattice constants shown in Figs. 1(c)–1(d).

Because the situation is basically similar between $n = 1$ and $n = \infty$, we just briefly show our calculation results. Figure 7 presents the calculated band structure of Sr_2VO_4 and Sr_2VO_3H. We can find some features similar to the $n = \infty$ case: strong entanglement of the t_{2g} and e_g bands, and a large energy separation between the V-d and anion bands. As a result, the screening interaction of Sr_2VO_3H is weaker in the t_{2g} model but stronger in the d model, compared with Sr_2VO_4. An extended nature of the $d_{3x^2-r^2}$ orbital, which

TABLE III. Hopping and interaction parameters (in eV) for the d model. The d_{xz} orbital in Sr_2VO_4 is omitted in this table since it is equivalent to the d_{yz} orbital.

		t_x	t_y	Δ	$U_d^{\rm scr}$	$U_d^{\rm bare}$
Sr_2VO_4	d_{xy}	−0.27	−0.27		3.48	15.95
	d_{yz}	−0.04	−0.24	−0.02	3.27	15.19
	$d_{y^2-z^2}$	−0.01	−0.47	2.61	3.33	15.13
	$d_{3x^2-r^2}$	−0.65	−0.18	2.73	3.49	15.98
Sr_2VO_3H	d_{xy}	0.09	−0.45		3.60	15.20
	d_{yz}	−0.06	−0.25	0.38	3.70	15.49
	d_{xz}	0.14	0.03	−0.07	3.36	14.25
	$d_{y^2-z^2}$	0.00	−0.43	2.91	3.86	16.04
	$d_{3x^2-r^2}$	0.88	−0.09	1.90	3.14	13.56

TABLE IV. Hopping and interaction parameters (in eV) for the t_{2g} model. The d_{xz} orbital in Sr_2VO_4 is omitted in this table since it is equivalent to the d_{yz} orbital. *: constrained LDA combined with the *GW* method. **: averaged over the orbitals.

		t_x	t_y	Δ	$U^{\rm scr}_{t_{2g}}$	$U^{\rm bare}_{t_{2g}}$
Sr_2VO_4	d_{xy}	−0.27	−0.27		3.46	15.91
					2.77* [55,56]	
					3.1** [51]	
	d_{yz}	−0.04	−0.24	−0.02	3.26	15.18
					2.58* [55,56]	
					3.1** [51]	
Sr_2VO_3H	d_{xy}	0.10	−0.44		2.51	14.93
	d_{yz}	−0.06	−0.25	0.39	2.84	15.25
	d_{xz}	0.14	0.03	−0.05	2.46	14.26

forms a chemical bond with the H-*s* orbital, is also realized in Sr_2VO_3H. In fact, Table III shows that both $U_d^{\rm scr}$ and $U_d^{\rm bare}$ exhibit small values for the the $d_{3x^2-r^2}$ orbital in Sr_2VO_3H.

One important difference between $n = 1$ and $n = \infty$ is the dimensionality of the electronic structure. As shown in Table IV, one can see that the hopping parameter along the x direction, t_x, is actually suppressed in $SrVO_3H$, where the hydrogen atom breaks a chemical bond between the V-t_{2g} orbitals. In addition, the layered structure cannot yield a large t_z both for Sr_2VO_4 and Sr_2VO_3H. Therefore, the t_{2g} orbitals in Sr_2VO_3H have a peculiar dimensionality. As for the d_{xy} orbital, its hopping parameters are quite similar to those for the d_{yz} orbital in $SrVO_2H$ shown in Table I. In other words, the d_{xy} orbital in Sr_2VO_3H has quasi-one-dimensional electronic structure with an enhanced hopping amplitude along the y direction. As for the d_{yz} orbital, it is less affected by the existence of hydrogen atoms, except for the on-site energy difference with the d_{xy} orbital, Δ, as shown in Table IV. The d_{xz} orbital in Sr_2VO_3H has a small hopping amplitude for all the directions, which is unique for $n = 1$.

V. CONCLUSION

We have derived several kinds of low-energy effective models for vanadium oxyhydrides $Sr_{n+1}V_nO_{2n+1}H_n$ ($n = 1, \infty$) and some oxides: $SrVO_3$, $SrCrO_3$, and Sr_2VO_4, using cRPA. We have found that, in $SrVO_2H$, (1) the e_g bands strongly entangled with the t_{2g} bands sizably screen the effective interaction in the t_{2g} model, (2) the large energy separation between the anion bands and the V-*d* bands weakens the screening effect by the anion orbitals in the *d* model (and the t_{2g} model), and (3) the strong entanglement of the V-*d* bands and higher-energy bands yields the strong screening effect in the *dps* model (and other two effective models). A similar tendency can be seen also in Sr_2VO_3H. Investigation of possible unique correlation effects in vanadium oxyhydrides based on the low-energy effective models derived in the present study is an open and interesting future study.

ACKNOWLEDGMENTS

Some calculations were performed using large-scale computer systems in the supercomputer center of the Institute for Solid State Physics, the University of Tokyo, and those of the Cybermedia Center, Osaka University. This study was supported by JSPS KAKENHI (Grants No. JP16H04338, No. JP17H05481, No. JP18H01860, and No. JP18K13470), Japan.

APPENDIX A: HOPPING PARAMETERS

The orbital index runs as (d_{xy}, d_{yz}, d_{xz}) for the t_{2g} model, and (d_{xy}, d_{yz}, d_{xz}, $d_{x^2-y^2}$, $d_{3z^2-r^2}$) for the *d* model, unless noted. The hopping parameters are defined for the (noninteracting) tight-binding Hamiltonian:

$$\mathcal{H}_0 = \sum_{ij} t_{ij}(\mathbf{R})\hat{c}_i^\dagger \hat{c}_j, \tag{A1}$$

where i and j are orbital indices. For clarity, we represent the lattice vector $\mathbf{R}$ with the Cartesian coordinate defined in Fig. 1. For the t_{2g} and *d* models, we denote the hopping matrix as $t^{t_{2g}}(R_x, R_y, R_z)$ and $t^{d}(R_x, R_y, R_z)$, respectively.

Some equivalent parameters are omitted here. For example, in $SrVO_3$, $t^{t_{2g}}(a, 0, 0)$, $t^{t_{2g}}(0, a, 0)$, and $t^{t_{2g}}(0, 0, a)$ are equivalent if the orbital indices are appropriately exchanged, and thus we only show one of them. For all the compounds investigated in this study, the d_{xy} on-site energy is set to zero.

1. $SrVO_3$

$$t^{t_{2g}}(0,0,0) = \begin{pmatrix} 0 & 0 & 0 \\ 0 & 0 & 0 \\ 0 & 0 & 0 \end{pmatrix}, \tag{A2}$$

$$t^{t_{2g}}(a,0,0) = \begin{pmatrix} -0.263 & 0 & 0 \\ 0 & -0.027 & 0 \\ 0 & 0 & -0.263 \end{pmatrix}, \tag{A3}$$

$$t^{t_{2g}}(a,a,0) = \begin{pmatrix} -0.084 & 0 & 0 \\ 0 & 0.006 & 0.009 \\ 0 & 0.009 & 0.006 \end{pmatrix}, \tag{A4}$$

$$t^d(0,0,0) = \begin{pmatrix} 0 & 0 & 0 & 0 & 0 \\ 0 & 0 & 0 & 0 & 0 \\ 0 & 0 & 0 & 0 & 0 \\ 0 & 0 & 0 & 2.765 & 0 \\ 0 & 0 & 0 & 0 & 2.765 \end{pmatrix}, \tag{A5}$$

$$t^d(a,0,0) = \begin{pmatrix} -0.262 & 0 & 0 & 0 & 0 \\ 0 & -0.025 & 0 & 0 & 0 \\ 0 & 0 & -0.262 & 0 & 0 \\ 0 & 0 & 0 & -0.505 & 0.293 \\ 0 & 0 & 0 & 0.293 & -0.167 \end{pmatrix}, \tag{A6}$$

$$t^d(0,0,a) = \begin{pmatrix} -0.025 & 0 & 0 & 0 & 0 \\ 0 & -0.262 & 0 & 0 & 0 \\ 0 & 0 & -0.262 & 0 & 0 \\ 0 & 0 & 0 & 0.003 & 0 \\ 0 & 0 & 0 & 0 & -0.674 \end{pmatrix}, \tag{A7}$$

$$t^d(2a,0,0) = \begin{pmatrix} 0.005 & 0 & 0 & 0 & 0 \\ 0 & 0.001 & 0 & 0 & 0 \\ 0 & 0 & 0.005 & 0 & 0 \\ 0 & 0 & 0 & -0.039 & 0.023 \\ 0 & 0 & 0 & 0.023 & -0.013 \end{pmatrix}, \tag{A8}$$

$$t^d(0,0,2a) = \begin{pmatrix} 0.001 & 0 & 0 & 0 & 0 \\ 0 & 0.005 & 0 & 0 & 0 \\ 0 & 0 & 0.005 & 0 & 0 \\ 0 & 0 & 0 & 0.000 & 0 \\ 0 & 0 & 0 & 0 & -0.052 \end{pmatrix}, \tag{A9}$$

$$t^d(a,a,0) = \begin{pmatrix} -0.083 & 0 & 0 & 0 & -0.031 \\ 0 & 0.006 & 0.010 & 0 & 0 \\ 0 & 0.010 & 0.006 & 0 & 0 \\ 0 & 0 & 0 & 0.041 & 0 \\ -0.031 & 0 & 0 & 0 & -0.017 \end{pmatrix}, \tag{A10}$$

$$t^d(a,0,a) = \begin{pmatrix} 0.006 & 0.010 & 0 & 0 & 0 \\ 0.010 & 0.006 & 0 & 0 & 0 \\ 0 & 0 & -0.083 & 0.027 & 0.015 \\ 0 & 0 & 0.027 & -0.002 & -0.025 \\ 0 & 0 & 0.015 & -0.025 & 0.027 \end{pmatrix}. \tag{A11}$$

2. $SrVO_2H$

$$t^{t_{2g}}(0,0,0) = \begin{pmatrix} 0 & 0 & 0 \\ 0 & -0.454 & 0 \\ 0 & 0 & -0.454 \end{pmatrix}, \tag{A12}$$

$$t^{t_{2g}}(a,0,0) = \begin{pmatrix} -0.251 & 0 & 0 \\ 0 & 0.012 & 0 \\ 0 & 0 & -0.423 \end{pmatrix}, \tag{A13}$$

$$t^{t_{2g}}(0,0,c) = \begin{pmatrix} -0.040 & 0 & 0 \\ 0 & 0.097 & 0 \\ 0 & 0 & 0.097 \end{pmatrix}, \tag{A14}$$

$$t^{t_{2g}}(0,0,2c) = \begin{pmatrix} -0.001 & 0 & 0 \\ 0 & 0.017 & 0 \\ 0 & 0 & 0.017 \end{pmatrix}, \tag{A15}$$

$$t^{t_{2g}}(a,a,0) = \begin{pmatrix} -0.068 & 0 & 0 \\ 0 & 0.013 & 0.027 \\ 0 & 0.027 & 0.013 \end{pmatrix}, \tag{A16}$$

$$t^{t_{2g}}(a,0,c) = \begin{pmatrix} 0.002 & -0.009 & 0 \\ -0.009 & -0.010 & 0 \\ 0 & 0 & 0.027 \end{pmatrix}, \tag{A17}$$

$$t^{d}(0,0,0) = \begin{pmatrix} 0 & 0 & 0 & 0 & 0 \\ 0 & -0.443 & 0 & 0 & 0 \\ 0 & 0 & -0.443 & 0 & 0 \\ 0 & 0 & 0 & 2.489 & 0 \\ 0 & 0 & 0 & 0 & 1.523 \end{pmatrix}, \tag{A18}$$

$$t^{d}(a,0,0) = \begin{pmatrix} -0.251 & 0 & 0 & 0 & 0 \\ 0 & 0.008 & 0 & 0 & 0 \\ 0 & 0 & -0.424 & 0 & 0 \\ 0 & 0 & 0 & -0.438 & 0.183 \\ 0 & 0 & 0 & 0.183 & -0.094 \end{pmatrix}, \tag{A19}$$

$$t^{d}(0,0,c) = \begin{pmatrix} -0.040 & 0 & 0 & 0 & 0 \\ 0 & 0.096 & 0 & 0 & 0 \\ 0 & 0 & 0.096 & 0 & 0 \\ 0 & 0 & 0 & 0.012 & 0 \\ 0 & 0 & 0 & 0 & 0.876 \end{pmatrix}, \tag{A20}$$

$$t^{d}(2a,0,0) = \begin{pmatrix} 0.009 & 0 & 0 & 0 & 0 \\ 0 & 0.001 & 0 & 0 & 0 \\ 0 & 0 & -0.017 & 0 & 0 \\ 0 & 0 & 0 & -0.035 & 0.020 \\ 0 & 0 & 0 & 0.020 & -0.004 \end{pmatrix}, \tag{A21}$$

$$t^{d}(0,0,2c) = \begin{pmatrix} -0.001 & 0 & 0 & 0 & 0 \\ 0 & 0.010 & 0 & 0 & 0 \\ 0 & 0 & 0.010 & 0 & 0 \\ 0 & 0 & 0 & -0.001 & 0 \\ 0 & 0 & 0 & 0 & -0.059 \end{pmatrix}, \tag{A22}$$

$$t^{d}(a,a,0) = \begin{pmatrix} -0.068 & 0 & 0 & 0 & -0.007 \\ 0 & 0.013 & 0.022 & 0 & 0 \\ 0 & 0.022 & 0.013 & 0 & 0 \\ 0 & 0 & 0 & 0.058 & 0 \\ -0.007 & 0 & 0 & 0 & -0.041 \end{pmatrix}, \tag{A23}$$

$$t^d(a,0,c) = \begin{pmatrix} 0.002 & -0.010 & 0 & 0 & 0 \\ -0.010 & -0.010 & 0 & 0 & 0 \\ 0 & 0 & 0.027 & -0.014 & -0.084 \\ 0 & 0 & -0.014 & 0.001 & 0.054 \\ 0 & 0 & -0.084 & 0.054 & -0.064 \end{pmatrix}, \tag{A24}$$

$$t^d(0,0,3c) = \begin{pmatrix} 0.000 & 0 & 0 & 0 & 0 \\ 0 & 0.000 & 0 & 0 & 0 \\ 0 & 0 & 0.000 & 0 & 0 \\ 0 & 0 & 0 & 0.001 & 0 \\ 0 & 0 & 0 & 0 & 0.011 \end{pmatrix}, \tag{A25}$$

$$t^d(a,0,2c) = \begin{pmatrix} 0.000 & -0.001 & 0 & 0 & 0 \\ -0.001 & -0.001 & 0 & 0 & 0 \\ 0 & 0 & 0.001 & -0.001 & 0.015 \\ 0 & 0 & -0.001 & 0.001 & 0.000 \\ 0 & 0 & 0.015 & 0.000 & -0.030 \end{pmatrix}, \tag{A26}$$

$$t^d(a,a,c) = \begin{pmatrix} -0.006 & -0.004 & -0.004 & 0 & 0.001 \\ -0.004 & -0.010 & 0.006 & -0.009 & 0.015 \\ -0.004 & 0.006 & -0.010 & 0.009 & 0.015 \\ 0 & -0.009 & 0.009 & -0.011 & 0 \\ 0.001 & 0.015 & 0.015 & 0 & -0.027 \end{pmatrix}. \tag{A27}$$

3. $SrCrO_3$

$$t^{t_{2g}}(0,0,0) = \begin{pmatrix} 0 & 0 & 0 \\ 0 & 0 & 0 \\ 0 & 0 & 0 \end{pmatrix}, \tag{A28}$$

$$t^{t_{2g}}(a,0,0) = \begin{pmatrix} -0.236 & 0 & 0 \\ 0 & -0.022 & 0 \\ 0 & 0 & -0.236 \end{pmatrix}, \tag{A29}$$

$$t^{t_{2g}}(a,a,0) = \begin{pmatrix} -0.087 & 0 & 0 \\ 0 & 0.008 & 0.010 \\ 0 & 0.010 & 0.008 \end{pmatrix}, \tag{A30}$$

$$t^d(0,0,0) = \begin{pmatrix} 0 & 0 & 0 & 0 & 0 \\ 0 & 0 & 0 & 0 & 0 \\ 0 & 0 & 0 & 0 & 0 \\ 0 & 0 & 0 & 2.522 & 0 \\ 0 & 0 & 0 & 0 & 2.522 \end{pmatrix}, \tag{A31}$$

$$t^d(a,0,0) = \begin{pmatrix} -0.236 & 0 & 0 & 0 & 0 \\ 0 & -0.022 & 0 & 0 & 0 \\ 0 & 0 & -0.236 & 0 & 0 \\ 0 & 0 & 0 & -0.509 & 0.295 \\ 0 & 0 & 0 & 0.295 & -0.168 \end{pmatrix}, \tag{A32}$$

$$t^d(0,0,a) = \begin{pmatrix} -0.022 & 0 & 0 & 0 & 0 \\ 0 & -0.236 & 0 & 0 & 0 \\ 0 & 0 & -0.236 & 0 & 0 \\ 0 & 0 & 0 & 0.002 & 0 \\ 0 & 0 & 0 & 0 & -0.679 \end{pmatrix}, \tag{A33}$$

$$t^d(2a,0,0)=\begin{pmatrix}0.004 & 0 & 0 & 0 & 0\\ 0 & 0.000 & 0 & 0 & 0\\ 0 & 0 & 0.004 & 0 & 0\\ 0 & 0 & 0 & -0.045 & 0.026\\ 0 & 0 & 0 & 0.026 & -0.015\end{pmatrix}, \tag{A34}$$

$$t^d(0,0,2a)=\begin{pmatrix}0.000 & 0 & 0 & 0 & 0\\ 0 & 0.004 & 0 & 0 & 0\\ 0 & 0 & 0.004 & 0 & 0\\ 0 & 0 & 0 & 0.000 & 0\\ 0 & 0 & 0 & 0 & -0.060\end{pmatrix}, \tag{A35}$$

$$t^d(a,a,0)=\begin{pmatrix}-0.087 & 0 & 0 & 0 & -0.032\\ 0 & 0.008 & 0.010 & 0 & 0\\ 0 & 0.010 & 0.008 & 0 & 0\\ 0 & 0 & 0 & 0.044 & 0\\ -0.032 & 0 & 0 & 0 & -0.017\end{pmatrix}, \tag{A36}$$

$$t^d(a,0,a)=\begin{pmatrix}0.008 & 0.010 & 0 & 0 & 0\\ 0.010 & 0.008 & 0 & 0 & 0\\ 0 & 0 & -0.087 & 0.028 & 0.016\\ 0 & 0 & 0.028 & -0.001 & -0.026\\ 0 & 0 & 0.016 & -0.026 & 0.029\end{pmatrix}. \tag{A37}$$

4. Sr_2VO_4

$$t^{t_{2g}}(0,0,0)=\begin{pmatrix}0 & 0 & 0\\ 0 & -0.017 & 0\\ 0 & 0 & -0.017\end{pmatrix}, \tag{A38}$$

$$t^{t_{2g}}(a,0,0)=\begin{pmatrix}-0.272 & 0 & 0\\ 0 & -0.045 & 0\\ 0 & 0 & -0.240\end{pmatrix}, \tag{A39}$$

$$t^{t_{2g}}(2a,0,0)=\begin{pmatrix}0.006 & 0 & 0\\ 0 & 0.001 & 0\\ 0 & 0 & 0.023\end{pmatrix}, \tag{A40}$$

$$t^{t_{2g}}(a,a,0)=\begin{pmatrix}-0.082 & 0 & 0\\ 0 & 0.006 & 0.000\\ 0 & 0.000 & 0.006\end{pmatrix}, \tag{A41}$$

$$t^{t_{2g}}\left(\frac{a}{2},\frac{a}{2},\frac{c}{2}\right)=\begin{pmatrix}0.001 & 0.003 & 0.003\\ 0.003 & -0.015 & -0.011\\ 0.003 & -0.011 & -0.015\end{pmatrix}. \tag{A42}$$

For the d model in Sr_2VO_4, the orbital index runs as $(d_{xy}, d_{yz}, d_{xz}, d_{y^2-z^2}, d_{3x^2-r^2})$, in order to compare its effective interaction parameters with those for Sr_2VO_3H.

$$t^d(0,0,0)=\begin{pmatrix}0 & 0 & 0 & 0 & 0\\ 0 & -0.020 & 0 & 0 & 0\\ 0 & 0 & -0.020 & 0 & 0\\ 0 & 0 & 0 & 2.607 & -0.109\\ 0 & 0 & 0 & -0.109 & 2.733\end{pmatrix}, \tag{A43}$$

$$t^d(a,0,0) = \begin{pmatrix} -0.272 & 0 & 0 & 0 & 0 \\ 0 & -0.044 & 0 & 0 & 0 \\ 0 & 0 & -0.241 & 0 & 0 \\ 0 & 0 & 0 & -0.007 & 0.017 \\ 0 & 0 & 0 & 0.017 & -0.650 \end{pmatrix}, \tag{A44}$$

$$t^d(0,a,0) = \begin{pmatrix} -0.272 & 0 & 0 & 0 & 0 \\ 0 & -0.241 & 0 & 0 & 0 \\ 0 & 0 & -0.044 & 0 & 0 \\ 0 & 0 & 0 & -0.475 & 0.287 \\ 0 & 0 & 0 & 0.287 & -0.183 \end{pmatrix}, \tag{A45}$$

$$t^d(2a,0,0) = \begin{pmatrix} 0.005 & 0 & 0 & 0 & 0 \\ 0 & 0.001 & 0 & 0 & 0 \\ 0 & 0 & 0.022 & 0 & 0 \\ 0 & 0 & 0 & 0.000 & 0.002 \\ 0 & 0 & 0 & 0.002 & -0.051 \end{pmatrix}, \tag{A46}$$

$$t^d(0,2a,0) = \begin{pmatrix} 0.005 & 0 & 0 & 0 & 0 \\ 0 & 0.022 & 0 & 0 & 0 \\ 0 & 0 & 0.001 & 0 & 0 \\ 0 & 0 & 0 & -0.036 & 0.023 \\ 0 & 0 & 0 & 0.023 & -0.014 \end{pmatrix}, \tag{A47}$$

$$t^d(a,a,0) = \begin{pmatrix} -0.081 & 0 & 0 & 0.024 & 0.014 \\ 0 & 0.006 & 0.000 & 0 & 0 \\ 0 & 0.000 & 0.006 & 0 & 0 \\ 0.024 & 0 & 0 & 0.004 & -0.025 \\ 0.014 & 0 & 0 & -0.025 & 0.033 \end{pmatrix}, \tag{A48}$$

$$t^d\left(\frac{a}{2},\frac{a}{2},\frac{c}{2}\right) = \begin{pmatrix} 0.000 & 0.004 & 0.004 & -0.022 & -0.013 \\ 0.004 & -0.015 & -0.011 & -0.011 & -0.010 \\ 0.004 & -0.011 & -0.015 & -0.014 & -0.004 \\ -0.022 & -0.011 & -0.014 & -0.021 & -0.013 \\ -0.013 & -0.010 & -0.004 & -0.013 & -0.007 \end{pmatrix}. \tag{A49}$$

5. Sr_2VO_3H

$$t^{t_{2g}}(0,0,0) = \begin{pmatrix} 0 & 0 & 0 \\ 0 & 0.393 & 0 \\ 0 & 0 & -0.049 \end{pmatrix}, \tag{A50}$$

$$t^{t_{2g}}(a,0,0) = \begin{pmatrix} 0.096 & 0 & 0 \\ 0 & -0.056 & 0 \\ 0 & 0 & 0.135 \end{pmatrix}, \tag{A51}$$

$$t^{t_{2g}}(0,b,0) = \begin{pmatrix} -0.442 & 0 & 0 \\ 0 & -0.250 & 0 \\ 0 & 0 & 0.032 \end{pmatrix}, \tag{A52}$$

$$t^{t_{2g}}(2a,0,0) = \begin{pmatrix} 0.021 & 0 & 0 \\ 0 & 0.000 & 0 \\ 0 & 0 & 0.003 \end{pmatrix}, \tag{A53}$$

$$t^{t_{2g}}(0,2b,0) = \begin{pmatrix} -0.005 & 0 & 0 \\ 0 & 0.020 & 0 \\ 0 & 0 & 0.000 \end{pmatrix}, \tag{A54}$$

$$t^{t_{2g}}(a,b,0) = \begin{pmatrix} 0.025 & 0 & 0 \\ 0 & 0.003 & -0.020 \\ 0 & -0.020 & -0.029 \end{pmatrix}, \tag{A55}$$

$$t^{t_{2g}}\left(\frac{a}{2},\frac{b}{2},\frac{c}{2}\right) = \begin{pmatrix} 0.001 & -0.011 & 0.005 \\ -0.011 & -0.019 & -0.023 \\ 0.005 & -0.023 & -0.018 \end{pmatrix}. \tag{A56}$$

For the d model in Sr_2VO_3H, the orbital index runs as (d_{xy}, d_{yz}, d_{xz}, $d_{y^2-z^2}$, $d_{3x^2-r^2}$), where hydrogen atoms are aligned along the x direction. In this model, we also show the imaginary part of the hopping parameters because they become non-negligible amplitude for some matrix elements.

$$t^{d}(0,0,0) = \begin{pmatrix} 0 & 0 & 0 & 0 & 0.001-0.001i \\ 0 & 0.378 & 0 & 0 & 0 \\ 0 & 0 & -0.069 & 0 & 0.002 \\ 0 & 0 & 0 & 2.907 & -0.042-0.042i \\ 0.001+0.001i & 0 & 0.002 & -0.042+0.042i & 1.901 \end{pmatrix}, \tag{A57}$$

$$t^{d}(a,0,0) = \begin{pmatrix} 0.091 & 0 & 0 & 0 & 0.001 \\ 0 & -0.056 & 0 & 0 & 0 \\ 0 & 0 & 0.135 & 0 & 0.001 \\ 0 & 0 & 0 & 0 & -0.020-0.039i \\ 0.001 & 0 & 0.001 & -0.020+0.039i & 0.878 \end{pmatrix}, \tag{A58}$$

$$t^{d}(0,b,0) = \begin{pmatrix} -0.445 & 0 & 0 & 0 & 0 \\ 0 & -0.255 & 0 & 0 & 0 \\ 0 & 0 & 0.032 & 0 & 0 \\ 0 & 0 & 0 & -0.426 & 0.104+0.133i \\ 0 & 0 & 0 & 0.104-0.133i & -0.095 \end{pmatrix}, \tag{A59}$$

$$t^{d}(2a,0,0) = \begin{pmatrix} 0.011 & 0 & 0 & 0 & 0 \\ 0 & 0 & 0 & 0 & 0 \\ 0 & 0 & 0.003 & 0 & 0 \\ 0 & 0 & 0 & 0.003 & -0.005-0.006i \\ 0 & 0 & 0 & -0.005+0.006i & -0.055 \end{pmatrix}, \tag{A60}$$

$$t^{d}(0,2b,0) = \begin{pmatrix} -0.013 & 0 & 0 & 0 & 0 \\ 0 & 0.022 & 0 & 0 & 0 \\ 0 & 0 & 0 & 0 & 0 \\ 0 & 0 & 0 & -0.040 & 0.012+0.016i \\ 0 & 0 & 0 & 0.012-0.016i & -0.012 \end{pmatrix}, \tag{A61}$$

$$t^{d}(a,b,0) = \begin{pmatrix} 0.025 & 0 & 0 & -0.005-0.001i & -0.055-0.072i \\ 0 & 0.002 & -0.020 & 0 & 0 \\ 0 & -0.020 & -0.029 & 0 & 0 \\ -0.005+0.001i & 0 & 0 & -0.004 & 0.030+0.042i \\ -0.055+0.072i & 0 & 0 & 0.030-0.042i & -0.071 \end{pmatrix}, \tag{A62}$$

$$t^{d}\left(\frac{a}{2},\frac{b}{2},\frac{c}{2}\right) = \begin{pmatrix} 0 & -0.010 & 0.005 & 0.003 & 0.001+0.002i \\ -0.010 & -0.019 & -0.022 & -0.008 & 0.002+0.003i \\ 0.005 & -0.022 & -0.018 & -0.005 & -0.005-0.006i \\ 0.003 & -0.008 & -0.005 & -0.017 & -0.013-0.017i \\ 0.001-0.002i & 0.002-0.003i & -0.005+0.006i & -0.013+0.017i & -0.021 \end{pmatrix}. \tag{A63}$$

APPENDIX B: INTERACTION PARAMETERS

The orbital index runs as (d_{xy}, d_{yz}, d_{xz}) for the t_{2g} model, and (d_{xy}, d_{yz}, d_{xz}, $d_{x^2-y^2}$, $d_{3z^2-r^2}$) for the d model, unless noted.

1. $SrVO_3$

$$U_{t_{2g}}^{\mathrm{scr}} = \begin{pmatrix} 3.42 & 2.43 & 2.43 \\ 2.43 & 3.42 & 2.43 \\ 2.43 & 2.43 & 3.42 \end{pmatrix}, \tag{B1}$$

$$U_{t_{2g}}^{\mathrm{bare}} = \begin{pmatrix} 15.78 & 14.49 & 14.49 \\ 14.49 & 15.78 & 14.49 \\ 14.49 & 14.49 & 15.78 \end{pmatrix}, \tag{B2}$$

$$J_{t_{2g}}^{\mathrm{scr}} = \begin{pmatrix} 3.42 & 0.48 & 0.48 \\ 0.48 & 3.42 & 0.48 \\ 0.48 & 0.48 & 3.42 \end{pmatrix}, \tag{B3}$$

$$J_{t_{2g}}^{\mathrm{bare}} = \begin{pmatrix} 15.78 & 0.61 & 0.61 \\ 0.61 & 15.78 & 0.61 \\ 0.61 & 0.61 & 15.78 \end{pmatrix}, \tag{B4}$$

$$U_{d}^{\mathrm{scr}} = \begin{pmatrix} 3.43 & 2.44 & 2.44 & 2.81 & 2.37 \\ 2.44 & 3.43 & 2.44 & 2.48 & 2.70 \\ 2.44 & 2.44 & 3.43 & 2.48 & 2.70 \\ 2.81 & 2.48 & 2.48 & 3.57 & 2.43 \\ 2.37 & 2.70 & 2.70 & 2.43 & 3.57 \end{pmatrix}, \tag{B5}$$

$$U_{d}^{\mathrm{bare}} = \begin{pmatrix} 15.85 & 14.55 & 14.55 & 15.36 & 14.52 \\ 14.55 & 15.85 & 14.55 & 14.73 & 15.15 \\ 14.55 & 14.55 & 15.85 & 14.73 & 15.15 \\ 15.36 & 14.73 & 14.73 & 16.36 & 14.73 \\ 14.52 & 15.15 & 15.15 & 14.73 & 16.36 \end{pmatrix}, \tag{B6}$$

$$J_{d}^{\mathrm{scr}} = \begin{pmatrix} 3.43 & 0.48 & 0.48 & 0.33 & 0.53 \\ 0.48 & 3.43 & 0.48 & 0.48 & 0.38 \\ 0.48 & 0.48 & 3.43 & 0.48 & 0.38 \\ 0.33 & 0.48 & 0.48 & 3.57 & 0.57 \\ 0.53 & 0.38 & 0.38 & 0.57 & 3.57 \end{pmatrix}, \tag{B7}$$

$$J_{d}^{\mathrm{bare}} = \begin{pmatrix} 15.85 & 0.61 & 0.61 & 0.35 & 0.70 \\ 0.61 & 15.85 & 0.61 & 0.61 & 0.44 \\ 0.61 & 0.61 & 15.85 & 0.61 & 0.44 \\ 0.35 & 0.61 & 0.61 & 16.36 & 0.81 \\ 0.70 & 0.44 & 0.44 & 0.81 & 16.36 \end{pmatrix}. \tag{B8}$$

For the dp model, the orbital index runs as (d_{xy}, d_{yz}, d_{xz}, $d_{x^2-y^2}$, $d_{3z^2-r^2}$, O1-$p_{x,y,z}$, O2-$p_{x,y,z}$, O3-$p_{x,y,z}$), where O1, O2, and O3 atoms place next to the vanadium atom along the x, y, and z directions, respectively.

$$U_{dp}^{\mathrm{scr}} = \left(\begin{array}{ccccc|ccc|ccc|ccc} 11.41 & 10.01 & 10.01 & 11.02 & 10.31 & 3.62 & 3.08 & 3.04 & 3.08 & 3.62 & 3.04 & 2.87 & 2.87 & 3.32 \\ 10.01 & 11.41 & 10.01 & 10.49 & 10.84 & 3.32 & 2.87 & 2.87 & 3.04 & 3.62 & 3.08 & 3.04 & 3.08 & 3.62 \\ 10.01 & 10.01 & 11.41 & 10.49 & 10.84 & 3.62 & 3.04 & 3.08 & 2.87 & 3.32 & 2.87 & 3.08 & 3.04 & 3.62 \\ 11.02 & 10.49 & 10.49 & 12.64 & 10.83 & 3.68 & 3.10 & 3.08 & 3.10 & 3.68 & 3.08 & 2.89 & 2.89 & 3.37 \\ 10.31 & 10.84 & 10.84 & 10.83 & 12.64 & 3.47 & 2.95 & 2.96 & 2.95 & 3.47 & 2.96 & 3.16 & 3.16 & 3.79 \\ \hline 3.62 & 3.32 & 3.62 & 3.68 & 3.47 & 8.73 & 6.81 & 6.81 & 2.10 & 2.14 & 2.01 & 2.10 & 2.01 & 2.14 \\ 3.08 & 2.87 & 3.04 & 3.10 & 2.95 & 6.81 & 8.07 & 6.55 & 2.12 & 2.10 & 2.00 & 2.00 & 1.93 & 2.01 \\ 3.04 & 2.87 & 3.08 & 3.08 & 2.96 & 6.81 & 6.55 & 8.07 & 2.00 & 2.01 & 1.93 & 2.12 & 2.00 & 2.10 \\ \hline 3.08 & 3.04 & 2.87 & 3.10 & 2.95 & 2.10 & 2.12 & 2.00 & 8.07 & 6.81 & 6.55 & 1.93 & 2.00 & 2.01 \\ 3.62 & 3.62 & 3.32 & 3.68 & 3.47 & 2.14 & 2.10 & 2.01 & 6.81 & 8.73 & 6.81 & 2.01 & 2.10 & 2.14 \\ 3.04 & 3.08 & 2.87 & 3.08 & 2.96 & 2.01 & 2.00 & 1.93 & 6.55 & 6.81 & 8.07 & 2.00 & 2.12 & 2.10 \\ \hline 2.87 & 3.04 & 3.08 & 2.89 & 3.16 & 2.10 & 2.00 & 2.12 & 1.93 & 2.01 & 2.00 & 8.07 & 6.55 & 6.81 \\ 2.87 & 3.08 & 3.04 & 2.89 & 3.16 & 2.01 & 1.93 & 2.00 & 2.00 & 2.10 & 2.12 & 6.55 & 8.07 & 6.81 \\ 3.32 & 3.62 & 3.62 & 3.37 & 3.79 & 2.14 & 2.01 & 2.10 & 2.01 & 2.14 & 2.10 & 6.81 & 6.81 & 8.73 \end{array}\right), \tag{B9}$$

$$U_{dp}^{\mathrm{bare}} = \left(\begin{array}{ccccc|ccc|ccc|ccc} 19.36 & 17.72 & 17.72 & 19.28 & 18.28 & 7.88 & 7.10 & 7.04 & 7.10 & 7.88 & 7.04 & 6.72 & 6.72 & 7.39 \\ 17.72 & 19.36 & 17.72 & 18.53 & 19.03 & 7.39 & 6.72 & 6.72 & 7.04 & 7.88 & 7.10 & 7.04 & 7.10 & 7.88 \\ 17.72 & 17.72 & 19.36 & 18.53 & 19.03 & 7.88 & 7.04 & 7.10 & 6.72 & 7.39 & 6.72 & 7.10 & 7.04 & 7.88 \\ 19.28 & 18.53 & 18.53 & 21.31 & 19.16 & 8.05 & 7.17 & 7.15 & 7.17 & 8.05 & 7.15 & 6.75 & 6.75 & 7.46 \\ 18.28 & 19.03 & 19.03 & 19.16 & 21.31 & 7.66 & 6.88 & 6.90 & 6.88 & 7.66 & 6.90 & 7.30 & 7.30 & 8.24 \\ \hline 7.88 & 7.39 & 7.88 & 8.05 & 7.66 & 19.82 & 17.24 & 17.24 & 5.23 & 5.30 & 5.08 & 5.23 & 5.08 & 5.30 \\ 7.10 & 6.72 & 7.04 & 7.17 & 6.88 & 17.24 & 18.55 & 16.71 & 5.24 & 5.23 & 5.06 & 5.06 & 4.93 & 5.08 \\ 7.04 & 6.72 & 7.10 & 7.15 & 6.90 & 17.24 & 16.71 & 18.55 & 5.06 & 5.08 & 4.93 & 5.24 & 5.06 & 5.23 \\ \hline 7.10 & 7.04 & 6.72 & 7.17 & 6.88 & 5.23 & 5.24 & 5.06 & 18.55 & 17.24 & 16.71 & 4.93 & 5.06 & 5.08 \\ 7.88 & 7.88 & 7.39 & 8.05 & 7.66 & 5.30 & 5.23 & 5.08 & 17.24 & 19.82 & 17.24 & 5.08 & 5.23 & 5.30 \\ 7.04 & 7.10 & 6.72 & 7.15 & 6.90 & 5.08 & 5.06 & 4.93 & 16.71 & 17.24 & 18.55 & 5.06 & 5.24 & 5.23 \\ \hline 6.72 & 7.04 & 7.10 & 6.75 & 7.30 & 5.23 & 5.06 & 5.24 & 4.93 & 5.08 & 5.06 & 18.55 & 16.71 & 17.24 \\ 6.72 & 7.10 & 7.04 & 6.75 & 7.30 & 5.08 & 4.93 & 5.06 & 5.06 & 5.23 & 5.24 & 16.71 & 18.55 & 17.24 \\ 7.39 & 7.88 & 7.88 & 7.46 & 8.24 & 5.30 & 5.08 & 5.23 & 5.08 & 5.30 & 5.23 & 17.24 & 17.24 & 19.82 \end{array}\right). \tag{B10}$$

Because the off-site exchange interaction is less than 0.1 eV, we only show the on-site exchange terms here. For the V-d orbitals,

$$J_{dp}^{\mathrm{scr},d} = \begin{pmatrix} 11.41 & 0.71 & 0.71 & 0.48 & 0.85 \\ 0.71 & 11.41 & 0.71 & 0.76 & 0.57 \\ 0.71 & 0.71 & 11.41 & 0.76 & 0.57 \\ 0.48 & 0.76 & 0.76 & 12.64 & 0.91 \\ 0.85 & 0.57 & 0.57 & 0.91 & 12.64 \end{pmatrix}, \quad \text{(B11)}$$

$$J_{dp}^{\mathrm{bare},d} = \begin{pmatrix} 19.36 & 0.82 & 0.82 & 0.49 & 1.00 \\ 0.82 & 19.36 & 0.82 & 0.87 & 0.62 \\ 0.82 & 0.82 & 19.36 & 0.87 & 0.62 \\ 0.49 & 0.87 & 0.87 & 21.31 & 1.08 \\ 1.00 & 0.62 & 0.62 & 1.08 & 21.31 \end{pmatrix}. \quad \text{(B12)}$$

For the O1-p orbitals,

$$J_{dp}^{\mathrm{scr},p} = \begin{pmatrix} 8.73 & 0.80 & 0.80 \\ 0.80 & 8.07 & 0.76 \\ 0.80 & 0.76 & 8.07 \end{pmatrix}, \quad \text{(B13)}$$

$$J_{dp}^{\mathrm{bare},p} = \begin{pmatrix} 19.82 & 0.97 & 0.97 \\ 0.97 & 18.55 & 0.93 \\ 0.97 & 0.93 & 18.55 \end{pmatrix}. \quad \text{(B14)}$$

The on-site exchange terms for the O2 and O3 atoms are equivalent to the above ones by appropriately exchanging the orbital indices.

2. $SrVO_2H$

$$U_{t_{2g}}^{\mathrm{scr}} = \begin{pmatrix} 3.00 & 1.85 & 1.85 \\ 1.85 & 2.60 & 1.69 \\ 1.85 & 1.69 & 2.60 \end{pmatrix}, \quad \text{(B15)}$$

$$U_{t_{2g}}^{\mathrm{bare}} = \begin{pmatrix} 16.04 & 14.36 & 14.36 \\ 14.36 & 15.18 & 13.91 \\ 14.36 & 13.91 & 15.18 \end{pmatrix}, \quad \text{(B16)}$$

$$J_{t_{2g}}^{\mathrm{scr}} = \begin{pmatrix} 3.00 & 0.46 & 0.46 \\ 0.46 & 2.60 & 0.42 \\ 0.46 & 0.42 & 2.60 \end{pmatrix}, \quad \text{(B17)}$$

$$J_{t_{2g}}^{\mathrm{bare}} = \begin{pmatrix} 16.04 & 0.60 & 0.60 \\ 0.60 & 15.18 & 0.57 \\ 0.60 & 0.57 & 15.18 \end{pmatrix}, \quad \text{(B18)}$$

$$U_{d}^{\mathrm{scr}} = \begin{pmatrix} 3.97 & 2.88 & 2.88 & 3.30 & 2.55 \\ 2.88 & 3.75 & 2.79 & 2.88 & 2.78 \\ 2.88 & 2.79 & 3.75 & 2.88 & 2.78 \\ 3.30 & 2.88 & 2.88 & 4.04 & 2.57 \\ 2.55 & 2.78 & 2.78 & 2.57 & 3.26 \end{pmatrix}, \quad \text{(B19)}$$

$$U_{d}^{\mathrm{bare}} = \begin{pmatrix} 16.06 & 14.41 & 14.41 & 15.46 & 13.35 \\ 14.41 & 15.28 & 13.99 & 14.50 & 13.52 \\ 14.41 & 13.99 & 15.28 & 14.50 & 13.52 \\ 15.46 & 14.50 & 14.50 & 16.37 & 13.44 \\ 13.35 & 13.52 & 13.52 & 13.44 & 13.58 \end{pmatrix}, \quad \text{(B20)}$$

$$J_{d}^{\mathrm{scr}} = \begin{pmatrix} 3.97 & 0.49 & 0.49 & 0.34 & 0.47 \\ 0.49 & 3.75 & 0.45 & 0.47 & 0.32 \\ 0.49 & 0.45 & 3.75 & 0.47 & 0.32 \\ 0.34 & 0.47 & 0.47 & 4.04 & 0.51 \\ 0.47 & 0.32 & 0.32 & 0.51 & 3.26 \end{pmatrix}, \quad \text{(B21)}$$

$$J_{d}^{\mathrm{bare}} = \begin{pmatrix} 16.06 & 0.60 & 0.60 & 0.36 & 0.62 \\ 0.60 & 15.28 & 0.57 & 0.59 & 0.38 \\ 0.60 & 0.57 & 15.28 & 0.59 & 0.38 \\ 0.36 & 0.59 & 0.59 & 16.37 & 0.69 \\ 0.62 & 0.38 & 0.38 & 0.69 & 13.58 \end{pmatrix}. \quad \text{(B22)}$$

For the dps model, the orbital index runs as (d_{xy}, d_{yz}, d_{xz}, $d_{x^2-y^2}$, $d_{3z^2-r^2}$, O1-$p_{x,y,z}$, O2-$p_{x,y,z}$, H-s), where O1, O2, and H atoms place next to the vanadium atom along the x, y, and z directions, respectively.

$$U_{dps}^{\mathrm{scr}} = \left(\begin{array}{ccccc|ccc|ccc|c} 8.16 & 6.48 & 6.48 & 7.61 & 6.53 & 2.99 & 2.63 & 2.61 & 2.63 & 2.99 & 2.61 & 2.83 \\ 6.48 & 7.28 & 6.17 & 6.72 & 6.65 & 2.66 & 2.38 & 2.40 & 2.56 & 2.94 & 2.63 & 3.08 \\ 6.48 & 6.17 & 7.28 & 6.72 & 6.65 & 2.94 & 2.56 & 2.63 & 2.38 & 2.66 & 2.40 & 3.08 \\ 7.61 & 6.72 & 6.72 & 8.95 & 6.79 & 3.03 & 2.62 & 2.63 & 2.62 & 3.03 & 2.63 & 2.86 \\ 6.53 & 6.65 & 6.65 & 6.79 & 7.90 & 2.74 & 2.41 & 2.45 & 2.41 & 2.74 & 2.45 & 3.28 \\ \hline 2.99 & 2.66 & 2.94 & 3.03 & 2.74 & 7.60 & 6.02 & 6.07 & 1.85 & 1.87 & 1.78 & 1.91 \\ 2.63 & 2.38 & 2.56 & 2.62 & 2.41 & 6.02 & 7.44 & 6.01 & 1.87 & 1.85 & 1.77 & 1.81 \\ 2.61 & 2.40 & 2.63 & 2.63 & 2.45 & 6.07 & 6.01 & 7.58 & 1.77 & 1.78 & 1.71 & 1.89 \\ \hline 2.63 & 2.56 & 2.38 & 2.62 & 2.41 & 1.85 & 1.87 & 1.77 & 7.44 & 6.02 & 6.01 & 1.81 \\ 2.99 & 2.94 & 2.66 & 3.03 & 2.74 & 1.87 & 1.85 & 1.78 & 6.02 & 7.60 & 6.07 & 1.91 \\ 2.61 & 2.63 & 2.40 & 2.63 & 2.45 & 1.78 & 1.77 & 1.71 & 6.01 & 6.07 & 7.58 & 1.89 \\ \hline 2.83 & 3.08 & 3.08 & 2.86 & 3.28 & 1.91 & 1.81 & 1.89 & 1.81 & 1.91 & 1.89 & 6.44 \end{array}\right), \quad \text{(B23)}$$

$$U_{dps}^{\text{bare}} = \left(\begin{array}{ccccc|ccc|ccc|c} 18.59 & 16.32 & 16.32 & 18.57 & 16.59 & 7.64 & 6.92 & 6.88 & 6.92 & 7.64 & 6.88 & 7.06 \\ 16.32 & 17.02 & 15.67 & 17.06 & 16.58 & 7.06 & 6.46 & 6.48 & 6.80 & 7.55 & 6.89 & 7.44 \\ 16.32 & 15.67 & 17.02 & 17.06 & 16.58 & 7.55 & 6.80 & 6.89 & 6.46 & 7.06 & 6.48 & 7.44 \\ 18.57 & 17.06 & 17.06 & 20.55 & 17.39 & 7.79 & 6.97 & 6.97 & 6.97 & 7.79 & 6.97 & 7.11 \\ 16.59 & 16.58 & 16.58 & 17.39 & 18.26 & 7.20 & 6.51 & 6.57 & 6.51 & 7.20 & 6.57 & 7.77 \\ \hline 7.64 & 7.06 & 7.55 & 7.79 & 7.20 & 19.03 & 16.82 & 16.91 & 5.10 & 5.16 & 4.97 & 5.22 \\ 6.92 & 6.46 & 6.80 & 6.97 & 6.51 & 16.82 & 18.36 & 16.62 & 5.12 & 5.10 & 4.95 & 5.04 \\ 6.88 & 6.48 & 6.89 & 6.97 & 6.57 & 16.91 & 16.62 & 18.54 & 4.95 & 4.97 & 4.83 & 5.18 \\ \hline 6.92 & 6.80 & 6.46 & 6.97 & 6.51 & 5.10 & 5.12 & 4.95 & 18.36 & 16.82 & 16.62 & 5.04 \\ 7.64 & 7.55 & 7.06 & 7.79 & 7.20 & 5.16 & 5.10 & 4.97 & 16.82 & 19.03 & 16.91 & 5.22 \\ 6.88 & 6.89 & 6.48 & 6.97 & 6.57 & 4.97 & 4.95 & 4.83 & 16.62 & 16.91 & 18.54 & 5.18 \\ \hline 7.06 & 7.44 & 7.44 & 7.11 & 7.77 & 5.22 & 5.04 & 5.18 & 5.04 & 5.22 & 5.18 & 14.14 \end{array}\right). \quad \text{(B24)}$$

Because the off-site exchange interaction is less than 0.1 eV except that between the $d_{3z^2-r^2}$ and s orbitals, we only show the d-d, d-s, and p-p exchange terms here. For the V-d + H-s orbitals,

$$J_{dps}^{\text{scr},ds} = \left(\begin{array}{cccccc} 8.16 & 0.62 & 0.62 & 0.45 & 0.69 & 0.01 \\ 0.62 & 7.28 & 0.57 & 0.64 & 0.47 & 0.09 \\ 0.62 & 0.57 & 7.28 & 0.64 & 0.47 & 0.09 \\ 0.45 & 0.64 & 0.64 & 8.95 & 0.76 & 0.01 \\ 0.69 & 0.47 & 0.47 & 0.76 & 7.90 & 0.16 \\ \hline 0.01 & 0.09 & 0.09 & 0.01 & 0.16 & 6.44 \end{array}\right), \quad \text{(B25)}$$

$$J_{dps}^{\text{bare},ds} = \left(\begin{array}{cccccc} 18.59 & 0.73 & 0.73 & 0.47 & 0.84 & 0.02 \\ 0.73 & 17.02 & 0.69 & 0.77 & 0.53 & 0.15 \\ 0.73 & 0.69 & 17.02 & 0.77 & 0.53 & 0.15 \\ 0.47 & 0.77 & 0.77 & 20.55 & 0.92 & 0.01 \\ 0.84 & 0.53 & 0.53 & 0.92 & 18.26 & 0.25 \\ \hline 0.02 & 0.15 & 0.15 & 0.01 & 0.25 & 14.14 \end{array}\right). \quad \text{(B26)}$$

For the O1-p orbitals,

$$J_{dps}^{\text{scr},p} = \begin{pmatrix} 7.60 & 0.76 & 0.76 \\ 0.76 & 7.44 & 0.75 \\ 0.76 & 0.75 & 7.58 \end{pmatrix}, \quad \text{(B27)}$$

$$J_{dps}^{\text{bare},p} = \begin{pmatrix} 19.03 & 0.94 & 0.94 \\ 0.94 & 18.36 & 0.92 \\ 0.94 & 0.92 & 18.54 \end{pmatrix}. \quad \text{(B28)}$$

3. $SrCrO_3$

$$U_{t_{2g}}^{\text{scr}} = \begin{pmatrix} 2.97 & 2.00 & 2.00 \\ 2.00 & 2.97 & 2.00 \\ 2.00 & 2.00 & 2.97 \end{pmatrix}, \quad \text{(B29)}$$

$$U_{t_{2g}}^{\text{bare}} = \begin{pmatrix} 16.18 & 14.89 & 14.89 \\ 14.89 & 16.18 & 14.89 \\ 14.89 & 14.89 & 16.18 \end{pmatrix}, \quad \text{(B30)}$$

$$J_{t_{2g}}^{\text{scr}} = \begin{pmatrix} 2.97 & 0.45 & 0.45 \\ 0.45 & 2.97 & 0.45 \\ 0.45 & 0.45 & 2.97 \end{pmatrix}, \quad \text{(B31)}$$

$$J_{t_{2g}}^{\text{bare}} = \begin{pmatrix} 16.18 & 0.59 & 0.59 \\ 0.59 & 16.18 & 0.59 \\ 0.59 & 0.59 & 16.18 \end{pmatrix}, \quad \text{(B32)}$$

$$U_{d}^{\text{scr}} = \begin{pmatrix} 3.04 & 2.07 & 2.07 & 2.43 & 1.99 \\ 2.07 & 3.04 & 2.07 & 2.10 & 2.32 \\ 2.07 & 2.07 & 3.04 & 2.10 & 2.32 \\ 2.43 & 2.10 & 2.10 & 3.18 & 2.05 \\ 1.99 & 2.32 & 2.32 & 2.05 & 3.18 \end{pmatrix}, \quad \text{(B33)}$$

$$U_{d}^{\text{bare}} = \begin{pmatrix} 16.20 & 14.91 & 14.91 & 15.78 & 14.93 \\ 14.91 & 16.20 & 14.91 & 15.14 & 15.57 \\ 14.91 & 14.91 & 16.20 & 15.14 & 15.57 \\ 15.78 & 15.14 & 15.14 & 16.82 & 15.19 \\ 14.93 & 15.57 & 15.57 & 15.19 & 16.82 \end{pmatrix}, \quad \text{(B34)}$$

$$J_{d}^{\text{scr}} = \begin{pmatrix} 3.04 & 0.47 & 0.47 & 0.33 & 0.52 \\ 0.47 & 3.04 & 0.47 & 0.47 & 0.38 \\ 0.47 & 0.47 & 3.04 & 0.47 & 0.38 \\ 0.33 & 0.47 & 0.47 & 3.18 & 0.56 \\ 0.52 & 0.38 & 0.38 & 0.56 & 3.18 \end{pmatrix}, \quad \text{(B35)}$$

$$J_{d}^{\text{bare}} = \begin{pmatrix} 16.20 & 0.60 & 0.60 & 0.35 & 0.68 \\ 0.60 & 16.20 & 0.60 & 0.60 & 0.43 \\ 0.60 & 0.60 & 16.20 & 0.60 & 0.43 \\ 0.35 & 0.60 & 0.60 & 16.82 & 0.82 \\ 0.68 & 0.43 & 0.43 & 0.82 & 16.82 \end{pmatrix}. \quad \text{(B36)}$$

4. Sr_2VO_4

$$U_{t_{2g}}^{\mathrm{scr}} = \begin{pmatrix} 3.46 & 2.41 & 2.41 \\ 2.41 & 3.26 & 2.36 \\ 2.41 & 2.36 & 3.26 \end{pmatrix}, \tag{B37}$$

$$U_{t_{2g}}^{\mathrm{bare}} = \begin{pmatrix} 15.91 & 14.28 & 14.28 \\ 14.28 & 15.18 & 13.96 \\ 14.28 & 13.96 & 15.18 \end{pmatrix}, \tag{B38}$$

$$J_{t_{2g}}^{\mathrm{scr}} = \begin{pmatrix} 3.46 & 0.45 & 0.45 \\ 0.45 & 3.26 & 0.43 \\ 0.45 & 0.43 & 3.26 \end{pmatrix}, \tag{B39}$$

$$J_{t_{2g}}^{\mathrm{bare}} = \begin{pmatrix} 15.91 & 0.59 & 0.59 \\ 0.59 & 15.18 & 0.57 \\ 0.59 & 0.57 & 15.18 \end{pmatrix}. \tag{B40}$$

For the d model in Sr_2VO_4, the orbital index runs as (d_{xy}, d_{yz}, d_{xz}, $d_{y^2-z^2}$, $d_{3x^2-r^2}$), in order to compare its effective interaction parameters with those for Sr_2VO_3H.

$$U_{d}^{\mathrm{scr}} = \begin{pmatrix} 3.48 & 2.42 & 2.42 & 2.44 & 2.71 \\ 2.42 & 3.27 & 2.36 & 2.67 & 2.32 \\ 2.42 & 2.36 & 3.27 & 2.38 & 2.62 \\ 2.44 & 2.67 & 2.38 & 3.33 & 2.36 \\ 2.71 & 2.32 & 2.62 & 2.36 & 3.49 \end{pmatrix}, \tag{B41}$$

$$U_{d}^{\mathrm{bare}} = \begin{pmatrix} 15.95 & 14.31 & 14.31 & 14.22 & 15.04 \\ 14.31 & 15.19 & 13.97 & 14.47 & 14.09 \\ 14.31 & 13.97 & 15.19 & 13.89 & 14.66 \\ 14.22 & 14.47 & 13.89 & 15.13 & 14.04 \\ 15.04 & 14.09 & 14.66 & 14.04 & 15.98 \end{pmatrix}, \tag{B42}$$

$$J_{d}^{\mathrm{scr}} = \begin{pmatrix} 3.48 & 0.45 & 0.45 & 0.44 & 0.37 \\ 0.45 & 3.27 & 0.44 & 0.30 & 0.49 \\ 0.45 & 0.44 & 3.27 & 0.43 & 0.36 \\ 0.44 & 0.30 & 0.43 & 3.33 & 0.54 \\ 0.37 & 0.49 & 0.36 & 0.54 & 3.49 \end{pmatrix}, \tag{B43}$$

$$J_{d}^{\mathrm{bare}} = \begin{pmatrix} 15.95 & 0.59 & 0.59 & 0.57 & 0.43 \\ 0.59 & 15.19 & 0.57 & 0.33 & 0.67 \\ 0.59 & 0.57 & 15.19 & 0.57 & 0.42 \\ 0.57 & 0.33 & 0.57 & 15.13 & 0.79 \\ 0.43 & 0.67 & 0.42 & 0.79 & 15.98 \end{pmatrix}. \tag{B44}$$

5. Sr_2VO_3H

$$U_{t_{2g}}^{\mathrm{scr}} = \begin{pmatrix} 2.51 & 1.78 & 1.63 \\ 1.78 & 2.84 & 1.78 \\ 1.63 & 1.78 & 2.46 \end{pmatrix}, \tag{B45}$$

$$U_{t_{2g}}^{\mathrm{bare}} = \begin{pmatrix} 14.93 & 13.91 & 13.38 \\ 13.91 & 15.25 & 13.59 \\ 13.38 & 13.59 & 14.26 \end{pmatrix}, \tag{B46}$$

$$J_{t_{2g}}^{\mathrm{scr}} = \begin{pmatrix} 2.51 & 0.43 & 0.39 \\ 0.43 & 2.84 & 0.41 \\ 0.39 & 0.41 & 2.46 \end{pmatrix}, \tag{B47}$$

$$J_{t_{2g}}^{\mathrm{bare}} = \begin{pmatrix} 14.93 & 0.57 & 0.53 \\ 0.57 & 15.25 & 0.55 \\ 0.53 & 0.55 & 14.26 \end{pmatrix}. \tag{B48}$$

For the d model in Sr_2VO_3H, the orbital index runs as (d_{xy}, d_{yz}, d_{xz}, $d_{y^2-z^2}$, $d_{3x^2-r^2}$), where hydrogen atoms are aligned along the x direction.

$$U_{d}^{\mathrm{scr}} = \begin{pmatrix} 3.60 & 2.72 & 2.58 & 2.75 & 2.67 \\ 2.72 & 3.70 & 2.64 & 3.11 & 2.42 \\ 2.58 & 2.64 & 3.36 & 2.68 & 2.58 \\ 2.75 & 3.11 & 2.68 & 3.86 & 2.47 \\ 2.67 & 2.42 & 2.58 & 2.47 & 3.14 \end{pmatrix}, \tag{B49}$$

$$U_{d}^{\mathrm{bare}} = \begin{pmatrix} 15.20 & 14.14 & 13.49 & 14.32 & 13.48 \\ 14.14 & 15.49 & 13.68 & 15.03 & 13.12 \\ 13.49 & 13.68 & 14.25 & 13.88 & 13.05 \\ 14.32 & 15.03 & 13.88 & 16.04 & 13.31 \\ 13.48 & 13.12 & 13.05 & 13.31 & 13.56 \end{pmatrix}, \tag{B50}$$

$$J_{d}^{\mathrm{scr}} = \begin{pmatrix} 3.60 & 0.46 & 0.42 & 0.43 & 0.31 \\ 0.46 & 3.70 & 0.43 & 0.32 & 0.45 \\ 0.42 & 0.43 & 3.36 & 0.41 & 0.30 \\ 0.43 & 0.32 & 0.41 & 3.86 & 0.49 \\ 0.31 & 0.45 & 0.30 & 0.49 & 3.14 \end{pmatrix}, \tag{B51}$$

$$J_{d}^{\mathrm{bare}} = \begin{pmatrix} 15.20 & 0.58 & 0.54 & 0.57 & 0.37 \\ 0.58 & 15.49 & 0.56 & 0.34 & 0.60 \\ 0.54 & 0.56 & 14.25 & 0.55 & 0.36 \\ 0.57 & 0.34 & 0.55 & 16.04 & 0.68 \\ 0.37 & 0.60 & 0.36 & 0.68 & 13.56 \end{pmatrix}. \tag{B52}$$

[1] M. Imada, A. Fujimori, and Y. Tokura, Rev. Mod. Phys. **70**, 1039 (1998).

[2] J. G. Bednorz and K. A. Müller, Z. Phys. B **64**, 189 (1986).

[3] B. M. Tissue, K. M. Cirillo, J. C. Wright, M. Daeumling, and D. C. Larbalestier, Solid State Commun. **65**, 51 (1988).

[4] A. C. W. P. James, D. W. Murphy, and S. M. Zahurak, Nature (London) **338**, 240 (1989).

[5] M. Al-Mamouri, P. P. Edwards, C. Greaves, and M. Slaski, Nature (London) **369**, 382 (1994).

[6] Z. Hiroi, N. Kobayashi, and M. Takano, Nature (London) **371**, 139 (1994).

[7] R. K. Li and C. Greaves, Phys. Rev. B **62**, 3811 (2000).

[8] H. Kageyama, K. Hayashi, K. Maeda, J. P. Attfield, Z. Hiroi, J. M. Rondinelli, and K. R. Poeppelmeier, Nat. Commun. **9**, 772 (2018).

[9] S. Iimura, S. Matsuishi, H. Sato, T. Hanna, Y. Muraba, S. W. Kim, J. E. Kim, M. Takata, and H. Hosono, Nat. Commun. **3**, 943 (2012).

[10] M. Hiraishi, S. Iimura, K. M. Kojima, J. Yamaura, H. Hiraka, K. Ikeda, P. Miao, Y. Ishikawa, S. Torii, M. Miyazaki, I. Yamauchi, A. Koda, K. Ishii, M. Yoshida, J. Mizuki, R. Kadono, R. Kumai, T. Kamiyama, T. Otomo, Y. Murakami *et al.*, Nat. Phys. **10**, 300 (2014).

[11] Y. Kobayashi, O. J. Hernandez, T. Sakaguchi, T. Yajima, T. Roisnel, Y. Tsujimoto, M. Morita, Y. Noda, Y. Mogami, A. Kitada, M. Ohkura, S. Hosokawa, Z. Li, K. Hayashi, Y. Kusano, J. E. Kim, N. Tsuji, A. Fujiwara, Y. Matsushita, K. Yoshimura *et al.*, Nat. Mater. **11**, 507 (2012).

[12] T. Sakaguchi, Y. Kobayashi, T. Yajima, M. Ohkura, C. Tassel, F. Takeiri, S. Mitsuoka, H. Ohkubo, T. Yamamoto, J. E. Kim, N. Tsuji, A. Fujihara, Y. Matsushita, J. Hester, M. Avdeev, K. Ohoyama, and H. Kageyama, Inorg. Chem. **51**, 11371 (2012).

[13] T. Yamamoto, R. Yoshii, G. Bouilly, Y. Kobayashi, K. Fujita, Y. Kususe, Y. Matsushita, K. Tanaka, and H. Kageyama, Inorg. Chem. **54**, 1501 (2015).

[14] N. Masuda, Y. Kobayashi, O. Hernandez, T. Bataille, S. Paofai, H. Suzuki, C. Ritter, N. Ichijo, Y. Noda, K. Takegoshi, C. Tassel, T. Yamamoto, and H. Kageyama, J. Am. Chem. Soc. **137**, 15315 (2015).

[15] M. A. Hayward, E. Cussen, J. Claridge, M. Bieringer, M. Rosseinsky, C. Kiely, S. Blundell, I. Marshall, and F. Pratt, Science **295**, 1882 (2002).

[16] C. A. Bridges, G. R. Darling, M. A. Hayward, and M. J. Rosseinsky, J. Am. Chem. Soc. **127**, 5996 (2005).

[17] C. Tassel, Y. Goto, Y. Kuno, J. Hester, M. Green, Y. Kobayashi, and H. Kageyama, Angew. Chem., Int. Ed. **53**, 10377 (2014).

[18] C. Tassel, Y. Goto, D. Watabe, Y. Tang, H. Lu, Y. Kuno, F. Takeiri, T. Yamamoto, C. M. Brown, J. Hester, Y. Kobayashi, and H. Kageyama, Angew. Chem., Int. Ed. **55**, 9667 (2016).

[19] Y. Goto, C. Tassel, Y. Noda, O. Hernandez, C. J. Pickard, M. A. Green, H. Sakaebe, N. Taguchi, Y. Uchimoto, Y. Kobayashi, and H. Kageyama, Inorg. Chem. **56**, 4840 (2017).

[20] T. Pussacq, H. Kabbour, S. Colis, H. Vezin, S. Saitzek, O. Gardoll, C. Tassel, H. Kageyama, C. Laberty Robert, and O. Mentré, Chem. Mater. **29**, 1047 (2017).

[21] R. M. Helps, N. H. Rees, and M. A. Hayward, Inorg. Chem. **49**, 11062 (2010).

[22] T. Yamamoto, K. Shitara, S. Kitagawa, A. Kuwabara, M. Kuroe, K. Ishida, M. Ochi, K. Kuroki, K. Fujii, M. Yashima, C. M. Brown, H. Takatsu, C. Tassel, and H. Kageyama, Chem. Mater. **30**, 1566 (2018).

[23] F. D. Romero, A. Leach, J. S. Möller, F. Foronda, S. J. Blundell, and M. A. Hayward, Angew. Chem., Int. Ed. **53**, 7556 (2014).

[24] J. Bang, S. Matsuishi, H. Hiraka, F. Fujisaki, T. Otomo, S. Maki, J. Yamaura, R. Kumai, Y. Murakami, and H. Hosono, J. Am. Chem. Soc. **136**, 7221 (2014).

[25] T. Yamamoto, D. Zeng, T. Kawakami, V. Arcisauskaite, K. Yata, M. A. Patino, N. Izumo, J. E. McGrady, H. Kageyama, and M. A. Hayward, Nat. Commun. **8**, 1217 (2017).

[26] S. Biermann, J. Phys.: Condens. Matter. **26**, 173202 (2014).

[27] T. Katayama, A. Chikamatsu, K. Yamada, K. Shigematsu, T. Onozuka, M. Minohara, H. Kumigashira, E. Ikenaga, and T. Hasegawa, J. Appl. Phys. **120**, 085305 (2016).

[28] Y. Wei, H. Gui, X. Li, Z. Zhao, Y.-H. Zhao, and W. Xie, J. Phys.: Condens. Matter **27**, 206001 (2015).

[29] K. Liu, Y. Hou, X. Gong, and H. Xiang, Sci. Rep. **6**, 19653 (2016).

[30] M. Imada and T. Miyake, J. Phys. Soc. Jpn. **79**, 112001 (2010).

[31] F. Aryasetiawan, M. Imada, A. Georges, G. Kotliar, S. Biermann, and A. I. Lichtenstein, Phys. Rev. B **70**, 195104 (2004).

[32] K. Momma and F. Izumi, J. Appl. Crystallogr. **44**, 1272 (2011).

[33] E. Şaşıoğlu, C. Friedrich, and S. Blügel, Phys. Rev. B **83**, 121101(R) (2011).

[34] P. Giannozzi, S. Baroni, N. Bonini, M. Calandra, R. Car, C. Cavazzoni, D. Ceresoli, G. L. Chiarotti, M. Cococcioni, I. Dabo, A. Dal Corso, S. Fabris, G. Fratesi, S. de Gironcoli, R. Gebauer, U. Gerstmann, C. Gougoussis, A. Kokalj, M. Lazzeri, L. Martin-Samos *et al.*, J. Phys.: Condens. Matter **21**, 395502 (2009).

[35] P. Giannozzi, O. Andreussi, T. Brumme, O. Bunau, M. Buongiorno Nardelli, M. Calandra, R. Car, C. Cavazzoni, D. Ceresoli, M. Cococcioni, N. Colonna, I. Carnimeo, A. Dal Corso, S. de Gironcoli, P. Delugas, R. A. DiStasio, Jr., A. Ferretti, A. Floris, G. Fratesi, G. Fugallo *et al.*, J. Phys.: Condens. Matter **29**, 465901 (2017).

[36] J. P. Perdew, K. Burke, and M. Ernzerhof, Phys. Rev. Lett. **77**, 3865 (1996).

[37] D. R. Hamann, Phys. Rev. B **88**, 085117 (2013).

[38] M. J. van Setten, M. Giantomassi, E. Bousquet, M. J. Verstraete, D. R. Hamann, X. Gonze, and G.-M. Rignanese, Comput. Phys. Commun. **226**, 39 (2018).

[39] V. A. Fotiev, G. V. Bazuev, and V. G. Zubkov, Inorg. Mater. **23**, 895 (1987).

[40] B. L. Chamberland, Solid State Commun. **5**, 663 (1967).

[41] N. Marzari and D. Vanderbilt, Phys. Rev. B **56**, 12847 (1997).

[42] I. Souza, N. Marzari, and D. Vanderbilt, Phys. Rev. B **65**, 035109 (2001).

[43] K. Nakamura, Y. Nohara, Y. Yosimoto, and Y. Nomura, Phys. Rev. B **93**, 085124 (2016).

[44] K. Nakamura, Y. Yoshimoto, T. Kosugi, R. Arita, and M. Imada, J. Phys. Soc. Jpn. **78**, 083710 (2009).

[45] K. Nakamura, R. Arita, and M. Imada, J. Phys. Soc. Jpn. **77**, 093711 (2008).

[46] Y. Nohara, S. Yamamoto, and T. Fujiwara, Phys. Rev. B **79**, 195110 (2009).

[47] T. Fujiwara, S. Yamamoto, and Y. Ishii, J. Phys. Soc. Jpn. **72**, 777 (2003).

[48] L. Vaugier, H. Jiang, and S. Biermann, Phys. Rev. B **86**, 165105 (2012).

[49] Y. Nomura, M. Kaltak, K. Nakamura, C. Taranto, S. Sakai, A. Toschi, R. Arita, K. Held, G. Kresse, and M. Imada, Phys. Rev. B **86**, 085117 (2012).

[50] T. Miyake and F. Aryasetiawan, Phys. Rev. B **77**, 085122 (2008).

[51] M. Casula, Ph. Werner, L. Vaugier, F. Aryasetiawan, T. Miyake, A. J. Millis, and S. Biermann, Phys. Rev. Lett. **109**, 126408 (2012).

[52] F. Aryasetiawan, K. Karlsson, O. Jepsen, and U. Schönberger, Phys. Rev. B **74**, 125106 (2006).

[53] S. W. Jang, H. Sakakibara, H. Kino, T. Kotani, K. Kuroki, and M. J. Han, Sci. Rep. **6**, 33397 (2016).

[54] T. Miyake, F. Aryasetiawan, and M. Imada, Phys. Rev. B **80**, 155134 (2009).

[55] Y. Imai, I. Solovyev, and M. Imada, Phys. Rev. Lett. **95**, 176405 (2005).

[56] Y. Imai and M. Imada, J. Phys. Soc. Jpn. **75**, 094713 (2006).